DISSERTATIONES
CHIMICAE
UNIVERSITATIS
TARTUENSIS
219

ANDRE LEESMENT

Quantitative studies of Brønsted acidity in biphasic systems and gas-phase

DISSERTATIONES CHIMICAE UNIVERSITATIS TARTUENSIS

219

DISSERTATIONES CHIMICAE UNIVERSITATIS TARTUENSIS
219

ANDRE LEESMENT

Quantitative studies of Brønsted acidity in biphasic systems and gas-phase

UNIVERSITY OF TARTU
Press

Institute of Chemistry, Faculty of Science and Technology, University of Tartu, Estonia.

The dissertation is accepted for the commencement of the degree of Doctor of Philosophy in Chemistry on May 3rd, 2023, by the Council of Institute of Chemistry, University of Tartu.

Supervisor: professor Ivo Leito, PhD.
University of Tartu, Estonia

Opponent: professor Kiyohiko Sugano, PhD.
Ritsumeikan University, Japan

Commencement: 9. June, 2023, at 10:15, Auditorium 1020, Ravila 14a, Tartu

European Union
European Regional
Development Fund

Investing
in your future

ISSN 1406-0299 (print)
ISBN 978-9916-27-212-1 (print)
ISSN 2806-2159 (pdf)
ISBN 978-9916-27-213-8 (pdf)

University of Tartu Press
www.tyk.ee

CONTENTS

LIST OF ORIGINAL PUBLICATIONS

I. **A. Leesment**, I. Kaljurand, A. Trummal, A. Kütt, T. Netscher, W. Bonrath, I. Leito, “Validation and extension of the gas-phase superacidity scale”. *Rapid Commun. Mass Spectrom.* **2020**, *e8598*.

II. **A. Leesment**, S. Selberg, M. Tammiste, A. H. Vu, T. H. Nguyen, L. Taylor-King, I. Leito, “Quantifying Acidity in Heterogeneous Systems: Biphasic pK_a Values”. *Anal. Chem.* **2022**, *94*, 4059–4064

III. **A. Leesment**, S. Selberg, I. Leito, “NMR as biphasic pK_a measurement technique”. *J. Chem. Metrol.* **2023**, *2*, 60–67.

Author’s contribution:

I. Lead author in writing the manuscript. Performed all the gas-phase acidity measurements and most of the data treatment.

II. Lead author in writing the manuscript. Performed most of the pK_a^{ow} measurements and most of data treatment.

III. Lead author in writing the manuscript. Performed all of the pK_a^{ow} measurements and all of data treatment.

ABBREVIATIONS

DCE	1,2-dichloroethane
Et_4N^+	tetraethylammonium cation
FT-ICR-MS	Fourier’ transform ion cyclotron resonance mass spectroscopy
GA	gas-phase acidity
HEPES	4-(2-hydroxyethyl)-1-piperazineethanesulfonic acid
IMRE	ion-molecule reaction equilibrium
K_a	acid dissociation constant
$\log P_{ow}$	octanol:water partitioning coefficient
MeCN	acetonitrile
pK_a	negative logarithm of acid dissociation constant
pK_a^{ow}	negative logarithm of octanol:water biphasic acid dissociation constant
W1BD	Unrestricted Brückner Doubles variation of Weizmann-1 theory, computational method

1. INTRODUCTION

Brønsted acidity and basicity of molecules in different media have been in the focus of researchers for decades. However, there are still some problematic areas in the field of acid-base chemistry which require further research. For this study, two of such areas were identified.

One of the two main topics of this dissertation is gas-phase acidity. It represents intrinsic acidity of compounds as no solvent effects are present in the gas-phase. Therefore, gas-phase acidities have fundamental importance. In addition, heterolytic dissociation reaction in the gas-phase is rather straight-forward and the range of acidities in gas-phase is virtually unlimited. This means that gas-phase acidities are very useful for describing substituent effects as well as developing and testing computational methods. Comparisons of acidities in the gas phase and in solvent enables elucidating solvent effects. Gas-phase acidities of a myriad of medium-strong, as well as many of the weakest acids have been reliably measured.[1,2] On the other hand, computational studies show the gas-phase acidity scale can be extended significantly further towards higher acidities.[3,4] Moreover, the reliability of the reported experimental gas-phase acidities for many strong acids has been disputed, suggesting that they should be remeasured.[5]

The second area of focus is biphasic pK_a. Acidities, expressed as pK_a values, have been measured in a number of different solvents. The most common is obviously water,[6] but non-aqueous solvents, such as dimethylsulfoxide,[7] acetonitrile,[8] 1,2-dichloroethane[9] and others[6,10] have also been used. However, there is not much data available on the acidity in biphasic systems, such as ones consisting of an aqueous phase at equilibrium with a water-immiscible phase. Such systems are present in various applications, for example, liquid-liquid extraction,[11] phase-transfer catalysis[12] and sensor membranes.[13] In these systems, compounds often act as ligands or catalysts and their acid-base properties are often approximated from single-phase data, such as aqueous pK_a. Such an approach is too simplified due to the presence of various phase transfer processes. As a result, especially in case of more lipophilic compounds, significant amounts of compound may be dissolved in the water-immiscible phase, while bulk of solvated H^+ resides in the aqueous phase. The ionization state of an acid in the organic phase can be very different from what it is in water at the same pH. Recently, the biphasic pK_a concept was developed in order to more adequately describe acid-base properties in biphasic systems[14] and as the study demonstrates, biphasic pK_a can be vastly different from the corresponding aqueous pK_a. These results show that more research on biphasic pK_a values is required. Biphasic acidity is a novel concept and before the start of this dissertation there were no biphasic pK_a values available for uncharged acids.

This thesis aims to:

- improve the previous gas-phase acidity measurement method,
- provide revised gas-phase acidities for some of the strong acids for which the previous experimental gas-phase acidity is deemed questionable,
- extend the gas-phase acidity scale towards higher acidities,
- refine existing and develop new methods for measurement of octanol:water biphasic $\mathrm{p}K_\mathrm{a}$ ($\mathrm{p}K_\mathrm{a}^\mathrm{ow}$) values,
- provide $\mathrm{p}K_\mathrm{a}^\mathrm{ow}$ values for acids of various structures and properties.

2. LITERATURE OVERVIEW

2.1 Gas-phase acidity

The gas-phase acidity (*GA*) of an acid HA is defined as the Gibbs' free energy change (ΔG_a) of heterolytic dissociation of the acid (Eqs. 1–2).

$$\mathrm{HA} \overset{GA}{\rightleftarrows} \mathrm{A}^- + \mathrm{H}^+ \tag{1}$$

$$\Delta G_\mathrm{a} = GA = -RT\ln K_\mathrm{a} \tag{2}$$

Here, A^- represents its conjugate base. *GA* values are typically expressed in kcal·mol^{-1} and a lower *GA* value indicates stronger acidic properties of the compound. Examples of experimental *GA* values of various compounds: methane, 408.7 kcal·mol^{-1};[1] water, 383.7 kcal·mol^{-1};[1] hydrogen bromide, 318.3 kcal·mol^{-1}[1] and sulfuric acid, 302 kcal·mol^{-1}.[15] Gas-phase acidities can also be expressed in pK_a units (at 298.15 K, 1 kcal·mol^{-1} is equivalent to 0.73 pK_a units), based on Eq. 2.

In most cases, gas-phase acidity measurements are performed using Fourier transform ion cyclotron resonance (FT-ICR-MS) equilibrium method. This method allows for measurement of relative *GA* values, meaning that the result of a measurement is the difference of gas-phase acidities between two compounds. Based on many individual relative *GA* measurements, a self-consistent scale is compiled.[16] Absolute gas-phase acidities are obtained by anchoring this scale to the compound with the most reliable absolute *GA* value(s) available.[1] When using the FT-ICR-MS method, the acidities of the compounds measured against each other need to be similar, typically within 4 kcal·mol^{-1}. Therefore, the extension of the self-consistent scale can only be achieved stepwise through a number of measurements with acids of various gas-phase acidities.

Measurements of gas-phase acidities are significantly different from measurements of acidities (typically expressed as pK_a values) in a solvent. Both theoretical and experimental gas-phase acidities are typically (but not always[17]) obtained under high-vacuum conditions, where it is assumed that the interactions between molecules and ions of the acid have essentially no influence on the measured acidity. In order to be able to measure the acidity of a compound in the gas-phase, the compound needs to be sufficiently volatile, while in a solvent, the compound needs to be sufficiently soluble. In addition, the range of acidities that can be measured in the solvent is limited by the solvent's autoprotolysis. In gas-phase, the acidity of any compound with sufficient volatility can in principle be measured.

GA measurements are of fundamental significance as gas-phase acidities represent a quantification of compound's intrinsic acidity, free of any solvent effects. The differences between acidities in the gas phase are usually much larger than in a solvent,[18] (with rare exceptions[19]) i.e. the gas phase is the most differentiating "medium". The reason for this is that there is no solvation present in gas-phase and solvation effects typically increase the acidities of weaker acids more than the acidities of stronger acids, thereby compressing the range of acidities in solvent.

Knowing *GA* values and using them as references enables us to adequately understand and describe the effects solvents have on acid-base properties of compounds. Similarly, gas-phase acidities enable comparing the effects various substituents have on acidities without the simultaneous presence of solvent effects.[20] In addition, heterolytic dissociation reaction of an acid in the gas-phase is relatively straight-forward and therefore, suitable for a model reaction for the development and testing of computational methods.[21]

When describing solvent and substituent effects and developing computational methods, it is very useful to have data available for as wide as possible range of acidities. The low-acidity end of the scale has been well established as even the *GA* values of various alkanes, known to be very weak acids, have been measured.[2] However, it is clear that the experimental *GA* scale can be extended significantly further towards higher acidities than the most acidic compound currently on the scale, $(C_4F_9SO_2)_2NH$. The previously reported gas-phase acidity of this compound is 278.7 kcal·mol^{-1} although the reliability of this value as well as the gas-phase acidities of many other superacids, discussed in Chapter 2.4, has been called into question. In 1,2-dichloroethane, multiple compounds have been shown to be more acidic than $(C_4F_9SO_2)_2NH$.[9] There is some experimental evidence (although with large uncertainties involved) suggesting that undecachlorocarborane acid, $H(CHB_{11}Cl_{11})$, is more acidic than $(C_4F_9SO_2)_2NH$ in the gas-phase.[22] Theoretical calculations suggest that it could be possible to extend the gas-phase acidity even down to 200 kcal·mol^{-1} or below.[3,4] All these studies indicate that there is a need for a lot of experimental work in the superacidic part of the scale. However, experimentally extending the scale further is complicated. This is highlighted by the fact that until this work, $(C_4F_9SO_2)_2NH$ remained the most acidic compound on the self-consistent experimental gas-phase acidity scale since 1994,[16] even though its gas-phase acidity has been revised in a later study.[23]

Generally, the strategy of extending the gas-phase scale towards stronger acids to a large extent revolves around the discovery and design of types of compounds that have a suitable range of gas-phase acidities so that they can be measured against previously known strongest acids and at the same time, their properties (for example, volatility and thermal stability) must be suitable for the measurements itself. The acidity of the suitable types of compounds can often be fine-tuned with the introduction of various substituents, such as fluorocarbon chains of various lengths. However, at some point, it becomes impossible to significantly enhance the acidity simply by varying the substituents and new types of acids are needed in order to expand the scale further. As such, even minor extensions of the scale are important as the difference in acidity to a generally more acidic type of compounds is reduced, perhaps even to an extent that would yield this difference to be directly measurable or at least provide insight on what kind of acids could be used next for this purpose. All of this complicates the process of extending the gas-phase acidity scale towards higher acidities, making it also rather unpredictable at the same time.

The compounds measured in this study have *GA* values below 300 kcal·mol^{-1}.

2.2 Methods for determining gas-phase acidity

Gas-phase acidity measurements are typically performed using the FT-ICR-MS equilibrium method. FT-ICR-MS allows trapping ions in the vacuum system for several minutes (or even longer if necessary), have them equilibrate with vapors of neutrals and then subsequently detect the ions formed during the reaction, making it a suitable method for observing and measuring equilibrium constants of various gas-phase ion-molecule reactions.

The FT-ICR-MS measurement method of gas-phase acidities is relative – the acidities of two compounds are compared against each other, and the result of the measurement is the difference in the acidities of the two compounds (expressed as ΔGA or $\Delta\Delta G_a$). This means that in order to obtain absolute acidities, the ΔGA values measured using the FT-ICR method need to be anchored to one or more compounds with known absolute *GA* values. Typical measurement using this method uses the following steps (see also Fig. 1): (1) the samples containing compound(s) of interest are placed in a container that is suitable for the insertion to the high-vacuum system (for example, either via solid probe or volatile compound source), so that a stable and sufficient vapor pressure of the compounds in the ICR cell can be achieved; (2) stable and sufficient vapor pressures of the compounds are generated; (3) various settings (such as, for example, trapping plate voltages, electron ionization pulse length and amplitude voltage) are optimized to ensure highest possible quality of the mass spectra at various durations of ion trapping; (4) generation of ions, using the electron ionization method, and collection of mass spectra at various durations of ion trapping, which are needed to adequately describe the equilibrium, are collected; (5) calculating equilibrium constant and the difference in gas-phase acidity, using the estimated partial pressures of the acids and equilibrium intensities of their anions in the mass spectra (see Fig. 2). The specifics of the used measurement method depend heavily on the intricacies and capabilities of the instrumentation used.

For some compounds, gas-phase acidities can also be estimated from other thermodynamic data. This includes absolute values with very low uncertainties which can be used as a reference. One such example uses the negative ion thermochemistry cycle,[1] which relates the bond dissociation energy (*BDE*) of a neutral acid (HA) with its deprotonation enthalpy, the electron affinity of the radical (A), and the ionization energy (IE) of hydrogen atom, according to Eq. 3. Gas-phase acidity of the neutral acid can then be calculated from the defining equation (Eq. 4) of Gibbs free energy.

$$BDE(\mathrm{HA}) = \Delta H_{\mathrm{a}}(\mathrm{HA}) + EA(\mathrm{A}) - IE(\mathrm{H}) \tag{3}$$

$$\Delta G_{\mathrm{a}}(\mathrm{HA}) = \Delta H_{\mathrm{a}}(\mathrm{HA}) + T\Delta S_{\mathrm{a}}(\mathrm{HA}) \tag{4}$$

2.3 Superacids

The term “superacid” was introduced in 1927, referring to acid systems stronger than conventional mineral acids.[24] In 1960s, it was discovered that long-lived electron deficient cations, such as carbocations, could be obtained in such systems.[25] George Andrew Olah received a Nobel Prize in 1994 for his research in this field.

Superacid chemistry is rather diverse. The first known superacids were mainly inorganic, for example $HClO_4$ and HSO_3F. These compounds require extreme care when handling, as many of them are powerful oxidizers or readily liberate toxic gases, such as HF.[25] For many applications, organic superacids are preferred as their properties are often more suitable from many aspects (solubility, possibility to tone acidity, etc).[25] Probably the best known organic superacids are perfluoroalkanesulfonic acids, such as triflic acid, CF_3SO_3H.[26] There are also various solid superacids known, examples of these include zeolitic acids, polymeric resin sulfonic acids (polystyrenesulfonic acid complexed with $AlCl_3$) and perfluorinated polymer resin acids (Nafion).[27] However, accurately describing their acidity is complicated as the acidity of such materials is often not uniform.[25]

Superacids are used as catalysts in various reactions and processes. Use of superacids allows generation and stabilization of various cations. Under extremely acidic conditions, protosolvation of these cations occurs,[25] further increasing electron deficiency at the reaction As various examples show, without an appropriate level of acidity, transformations do not take place or occur at a much lower rate.[25] For example, straight-chain alkanes are among the major components of petroleum which are not desirable in gasoline due to their low octane number. Conversion reactions of these alkanes into branched-chain alkanes or olefins is often carried out at a large industrial scale, require acidic catalysts such as $AlCl_3$ (at around 100 ^{o}C) or noble metal catalysts (at 200–500 ^{o}C) in order to activate the C–H and C–C bonds.[25] In superacidic conditions, such conversions can take place even at temperatures below 0 ^{o}C.[25]

Superacid anions are very weak bases. Many of them are considered weakly-coordinating, as their charge is delocalized.[28] Some of them exhibit high thermal and electrochemical stability.[29,30] These properties have led to the use of superacid anions in ionic liquids and electrolytes in various devices such as supercapacitors and Li-ion batteries.[31–33]

In order to properly design and apply superacids, it is important to know their acidities. Gas-phase acidities serve as a reference, as they represent the compound’s intrinsic acidity without the presence of any solvent effects.

2.4 Gas-phase acidities of superacids

Gas-phase acidities of several superacids, defined as acids stronger than sulfuric acid in the respective medium, have been previously measured by Koppel *et al*,[16] Leito *et al*[34] and Zhang *et al.*[23] The reliability of some of the results has been disputed as in case of many strong acids, there is a significant difference between the reported experimental *GA* values and corresponding high-level computational *GA* values.[5,35] An important example of such acids is trifluoromethanesulfonic acid with experimental *GA* values of 299.5 kcal·mol^{-1} at 373 K[16] and 298.8 kcal·mol^{-1} at 368 K,[15] while its gas-phase acidity obtained using a high-accuracy computational method W1BD[36,37] is 291.3 kcal·mol^{-1} at 373.15 K (Publication I) or 292.7 kcal·mol^{-1} at 298.15 K.[35] Other computational methods have yielded *GA* values between 290 and 293 kcal·mol^{-1} for triflic acid.[5]

Discrepancies between experimental and computational values are most likely related mainly to uncertainty of the experimental values, as the standard uncertainty of values obtained using a high-level computational method (such as W1BD) can rather reliably be estimated to be approximately 1 kcal·mol^{-1}, even though the availability of gas-phase acidities obtained with this method is limited. For example, the root mean square difference of W1BD energy calculation results was 0.62 kcal·mol^{-1} compared to G2/97 experimental data set with a root mean square uncertainty of 0.48 kcal·mol^{-1}[36] and 1.4 kcal·mol^{-1} when compared to a set of 54 gas-phase enthalpies of formation.[37]

Individual relative *GA* measurements using the FT-ICR-MS can have uncertainties as low as 0.2 kcal.[1] However, in many cases, uncertainties can be significantly higher, mainly due to difficulties in obtaining accurate estimates of partial pressures of the two compounds in the ICR cell. When using the FT-ICR-MS method, the acidities of the two compounds need to be within 4 kcal·mol^{-1} in most cases. As the number of suitable reference compounds is limited, it is not possible to measure most acids directly against a reference compound with a directly determined absolute *GA* value. The previously reported *GA* scales[23,34,38] have been fundamentally anchored using the experimental absolute *GA* value of HBr (318.28 kcal·mol^{-1} at 298.15 K[1]), although in two out of three the anchor point was the *GA* value of an acid stronger than HBr, which itself has been anchored to the same HBr *GA* value. The uncertainty of the gas-phase acidity of HBr is estimated to be as low as 0.05 kcal mol^{-1}.[1] Therefore, HBr is a suitable reference acid. Unfortunately, gas-phase acidities with such accuracy are available only for compounds, for which reliable measurement of the corresponding homolytic bond dissociation energy is possible, such as hydrogen halogenides. This means that the choice of suitable reference acids is very limited.

The gas-phase acidity scale now stretches downwards by around 40 kcal mol^{-1} from HBr. This means that the acidities of the strongest acids have been obtained by combining tens of relative *GA* measurements. This leads to a significant extrapolation. True, numerous overlapping measurements have been carried out and this improves the reliability of the results. However, each measurement has uncertainty, making the combined uncertainty of the *GA* values of the strongest acids quite high. In this context, especially significant are uncertainty sources that lead to systematic contraction (less commonly expansion) of the scale.

As a part of this work, in order to improve the accuracy of Δ*GA* values, changes to the previously used measurement methods were introduced. In addition, the results are anchored to high-level computational *GA* values, rather than to experimental *GA* values as has been done previously. These changes are introduced in order to provide more reliable *GA* values than the ones previously reported.

2.5 Acid-base properties in biphasic systems

Quantification of acid-base properties in a single solvent is rather well established. Acidity and basicity of molecules are commonly expressed via $\mathrm{p}K_\mathrm{a}$, the negative logarithm of the equilibrium constant of the dissociation reaction of the acid, or in case of basicity, the conjugate acid of the base. Various methods have been developed for measuring $\mathrm{p}K_\mathrm{a}$ values,[39] including spectrophotometric,[18,40,41] potentiometric[42] and NMR spectroscopic[43] methods. $\mathrm{p}K_\mathrm{a}$ measurements have been carried out in a number of solvents, such as dimethylsulfoxide,[7] acetonitrile,[8] 1,2-dichloroethane[9] and, of course, water.[6,43]

It is much more complex and challenging to adequately describe acid-base properties in heterogenous systems. This is due to potential phase transfer processes but also because the properties (such as composition) of each of the phases contribute to the properties of the system as a whole. Acid-base equilibria often have a significant influence on various processes in heterogenous systems. Therefore, adequate quantification of acid-base properties of compounds in these systems is very important.

Biphasic systems, such as one consisting of an aqueous phase and a water-immiscible organic phase, are found in many applications, such as liquid extraction,[11] sensor membranes[12] and phase-transfer catalysis.[13] Various acids and bases often act as catalysts or ligands in these systems. However, their acid-base properties are usually estimated from the corresponding monophasic acidity data such as aqueous $\mathrm{p}K_\mathrm{a}$, as quantitative acidity-basicity measurements are nearly universally performed in monophasic conditions. Such approximation, especially in the case of more lipophilic compounds, can be erroneous, as lipophilic species, both neutrals and ions (as ion pairs) are predominantly dissolved in the low-polar non-aqueous phase. At the same time, the bulk of solvated H^+ ions are mainly present in the aqueous phase. Moreover, acid-base properties in biphasic systems involve ionization, distribution, dissociation, ion-pairing and migration between phases – many of these processes are either much simpler or not even relevant in a system consisting of one phase. Therefore, the common approach of describing a compound's biphasic acid-base properties using its single-phase $\mathrm{p}K_\mathrm{a}$ cannot be considered appropriate.

As the two phases in a biphasic system, such as one consisting of octanol and water, are in an equilibrium with each other, the chemical potential and therefore, thermodynamic activity, of the species, including solvated H^+, is equal in both phases. This means that the acidities of the phases are equal in terms of the unified pH (pH_abs).[44] Usually, the solvated H^+ concentration is significantly higher in the aqueous phase. At the same time, the activity of each individual solvated proton is much higher in the organic phase. This is due to protons in the organic phase being not as strongly solvated as those in the aqueous phase. All of this means that we can know the activity of H^+ in both phases simply by measuring it in one of the phases.[44]

Recently, a novel concept, termed as "biphasic pK_a", was introduced.[14] Biphasic pK_a enables quantifying acid-base properties in biphasic systems in a more realistic way by accounting for the distribution of the neutral and anion into the lipophilic phase. A preliminary measurement method was developed and applied on a few iminophosphorane bases in a system, which consisted of a 1-octanol phase at an equilibrium with an aqueous phase.[14] The ratio of the base and its conjugate acid was measured in the 1-octanol phase, using a UV-Vis spectrophotometric method. The activity of H^+ was measured in the aqueous phase with a conventional pH-meter. As a result of that study, it was discovered that the octanol:water biphasic pK_a values (pK_a^{ow}), were significantly (by 1.6 to 3.4 units) lower than the corresponding aqueous pK_a values.[14] These results highlight the dangers of using single-phase pK_a values for describing acid-base properties in biphasic systems.

Although biphasic pK_a values can be measured for various biphasic systems, the octanol:water biphasic pK_a values (pK_a^{ow}) are particularly relevant as octanol:water system is considered a suitable reference system for biological partitioning[45] and the most commonly used quantitative estimate of a compound's lipophilicity is its octanol-water partitioning coefficient, logP_{ow}.

As was explained above, using aqueous pK_a values to describe acid-base properties of compounds in biphasic systems is not a reasonable approach. However, the amount of available data of the more relevant pK_a^{ow} values is extremely limited. In particular, before the start of this work there were no pK_a^{ow} values available for uncharged (neutral) acids. In this work, the pK_a^{ow} measurement method is further developed and applied to the measurement of biphasic of a range of uncharged acids from different families.

3. EXPERIMENTAL SECTION

3.1 Instruments and equipment

FT-ICR-MS measurements
The measurements were performed on a Varian 930MS FT-ICR mass spectrometer with a 7 T superconducting magnet. A comprehensive description of this particular spectrometer is given by Kaljurand *et al.*[46] Varian Omega software was used for controlling the instrument and data acquisition.

NMR measurements
NMR measurements were performed on a Bruker Avance-III 700 NMR spectrometer (16.4 T, ^{1}H resonance frequency 700.1 MHz, ^{13}C resonance frequency 176.0 MHz, ^{19}F resonance frequency 658.7 MHz, ^{31}P resonance frequency 283.4 MHz). Measurements were carried out in water-saturated octanol at 25.0 ± 0.1 °C, using TopSpin 3.2.7 software. The largest peak of the spectrum (corresponding to $-CH_2$ hydrogens of carbons 3–7 in 1-octanol) was used for shimming. Calibration of spectra was performed as indicated in publications II and III.

UV-Vis measurements
UV-Vis spectrometric measurements were carried out at room temperature (23.0 ± 2.0 °C) on a Thermo Spectronic Evolution 300 double-beam spectrophotometer, using 10.00 mm quartz cuvettes. In measurements where the concentration of the acid of interest was in the sub-mM range, the wavelength for absorbance measurements was chosen so that the difference in molar absorptivities of the neutral acid and its conjugate base was maximal. At higher concentrations, the absorbances at these wavelengths were often significantly above the usually recommended maximum absorbance value of 1 absorbance unit (AU) and therefore, a longer wavelength (at which the maximum absorbance was below 1 AU) was chosen. Stock 1-octanol was used as the reference solution. One-point baseline correction was used.

pH measurements
pH was measured using a Mettler Toledo InLab Micro pH-sensor, which was calibrated using pH 4.00 and pH 7.00 buffers. A pH 10.00 buffer was used to verify the calibration (discrepancies usually did not exceed 0.03 pH units and never 0.05 pH units). Details of the buffer solutions used are given in publications II and III.

3.2 *GA* measurement method

The main principle of the used Fourier transform ion cyclotron resonance mass spectrometry (FT-ICR-MS) equilibrium gas-phase acidity measurement method was described in detail by Leito *et al.*[34] The vapors of the two acids were leaked into the ICR cell region kept at near 373 K. Compounds were introduced using either the specifically designed inlet system (volatile compound source) or the solid sample probes. The latter method allows introducing compounds of very low volatility. Anions of the acids were generated by low energy (typically -15 to -20V) electron impact ionization pulses. The formed ions were trapped in the ICR cell and allowed to react with the neutrals in the gas phase until equilibrium could be observed. Equilibrium is considered to be reached when equilibrium constants calculated from data obtained after a certain reaction time form a plateau. Partial pressures of the compounds (estimated from mass spectra, see below), denoted as $p(\mathrm{HA_1})$ and $p(\mathrm{HA_2})$; the equilibrium-state signal intensities of the anions, $I(\mathrm{A_1^-})$ and $I(\mathrm{A_2^-})$; isotopic abundances of the anions, $\sigma(\mathrm{A_1^-})$ and $\sigma(\mathrm{A_2^-})$; polarizabilities of the acids as a measure of the efficiency of electron ionization for these acids, $S_r(\mathrm{HA_1})$ and $S_r(\mathrm{HA_2})$, were the parameters used to calculate the equilibrium constant value (K) of the proton transfer reaction and ΔGA of the acids $\mathrm{HA_1}$ and $\mathrm{HA_2}$, using Eq 5–7. Details about these parameters are provided in SI of Publication I.

$$\mathrm{HA_1} + \mathrm{A_2^-} \overset{\Delta GA}{\rightleftarrows} \mathrm{HA_2} + \mathrm{A_1^-} \tag{5}$$

$$K = \frac{p(\mathrm{HA_2}) \cdot S_r(\mathrm{HA_1}) \cdot I(\mathrm{A_1^-}) \cdot \sigma(\mathrm{A_1^-})}{p(\mathrm{HA_1}) \cdot S_r(\mathrm{HA_2}) \cdot I(\mathrm{A_2^-}) \cdot \sigma(\mathrm{A_2^-})} \tag{6}$$

$$\Delta GA = -RT\ln K_\mathrm{a} \tag{7}$$

In the previous studies,[16,23,34] partial pressures of the neutrals were typically estimated from the pressure gauge readings. However, the results obtained using this approach were inconsistent, likely due to the lack of selectivity. When using this method, it is assumed that the changes in the total pressure of the high-vacuum system result from changes in the partial pressures of the compounds being measured. However, various volatile impurities, products of partial decomposition and previously measured compounds desorbed from the surfaces of the high-vacuum system may contribute significantly to the total pressure in the high-vacuum system, especially when their vapor pressure is much higher than the vapor pressure of the compound actually being measured. This can lead to seriously over-estimated partial pressures, possibly even by a several orders of magnitude. It is also worth noting that in order to obtain consistent readings, the pressure gauge needs to be placed relatively far from the ICR cell due to the presence of strong magnetic field in and around the ICR cell during measurements (see Fig. 1). It is likely that the changes of the pressure at the pressure gauge are different from the changes in the ICR cell.

Due to these reasons, short-reaction-time negative ion mass-spectra were used to estimate the ratio of partial pressures of the compounds. Based on the assumption that the main product of electron ionization of the strong acids with low-energy electron beam is the corresponding conjugate base,[16] the intensity ratio of the conjugate bases of the acids, obtained at various short reaction times, was extrapolated to zero reaction time and corrected with the same S_r

parameters as above. This method of estimating partial pressures yielded consistent measurement results and therefore, was used in this study. Negative ion mass spectra were more suitable for estimating the ratio of partial pressures than positive ion mass spectra because they were generally more straight-forward to interpret. This is at least partially due to higher intensities of the negative ion signals. Therefore, positive ion mass-spectra were not used for determination of partial pressure ratios. Further discussion of the method used to estimate partial pressures is provided in the SI of Publication I.

In order to show that proton transfer is reversible and true equilibrium is reached, the data was collected also under double resonance conditions, where all ions with the exception of the conjugate base of one of the acids were removed from the ICR cell (i.e., the conjugate base of the acid was isolated). In order to obtain signals of sufficient intensity, the removal of all other ions was performed usually 500 ms to 2 seconds after the start of the ionization pulse. Changes in the intensities of the conjugate bases under these conditions can clearly be attributed to proton transfer reactions. Ions were trapped in the ICR cell and allowed to react with the neutral species in the cell according to Eq. 5 until equilibrium could be observed under the double resonance conditions as well. Agreement between equilibrium constant values measured with and without the removal of ions confirms that true equilibrium state was indeed reached. Example of the data collected during a single measurement is shown on Fig. 2.

Details of the measurement method and the changes introduced to the previous method are further explained and rationalized in Publication I.

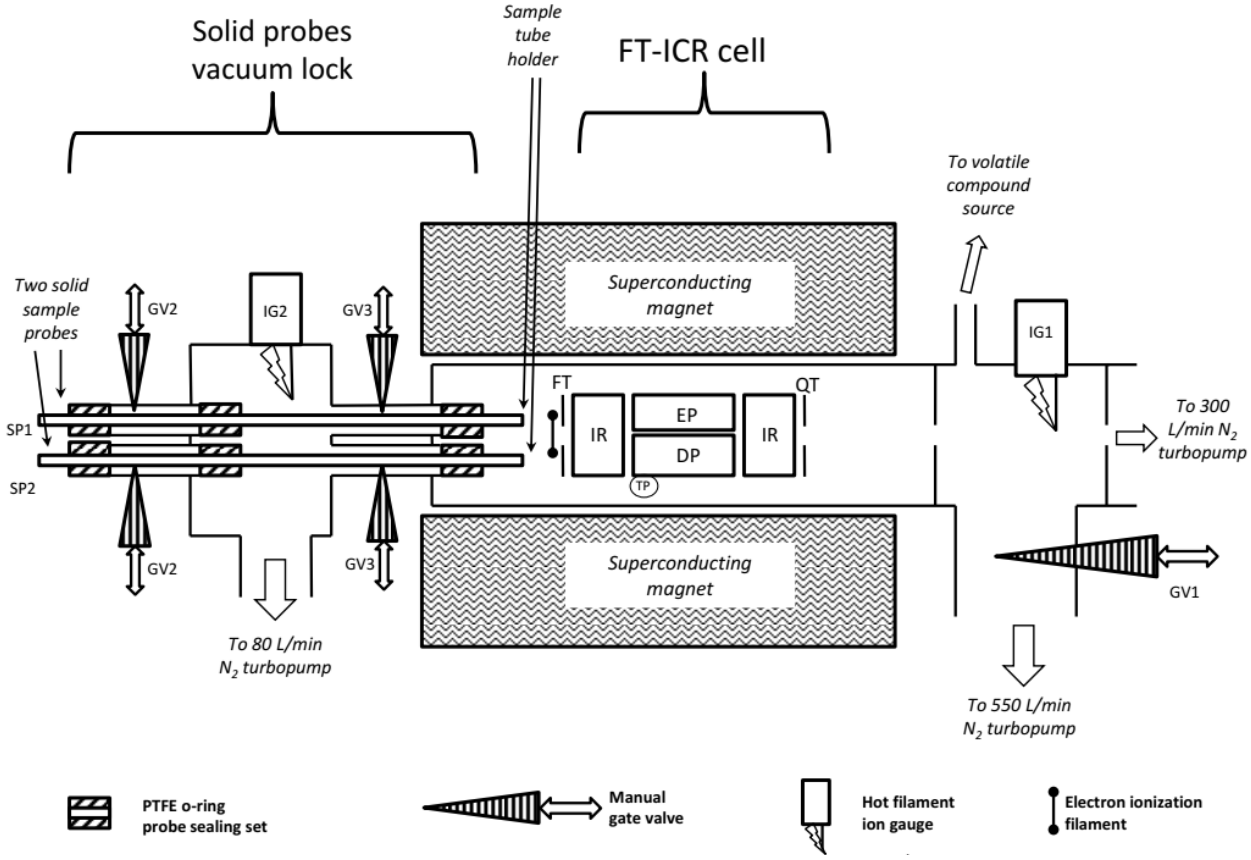

Figure 1. Principal scheme (when viewed from above) of the experimental setup used in this study.[46]

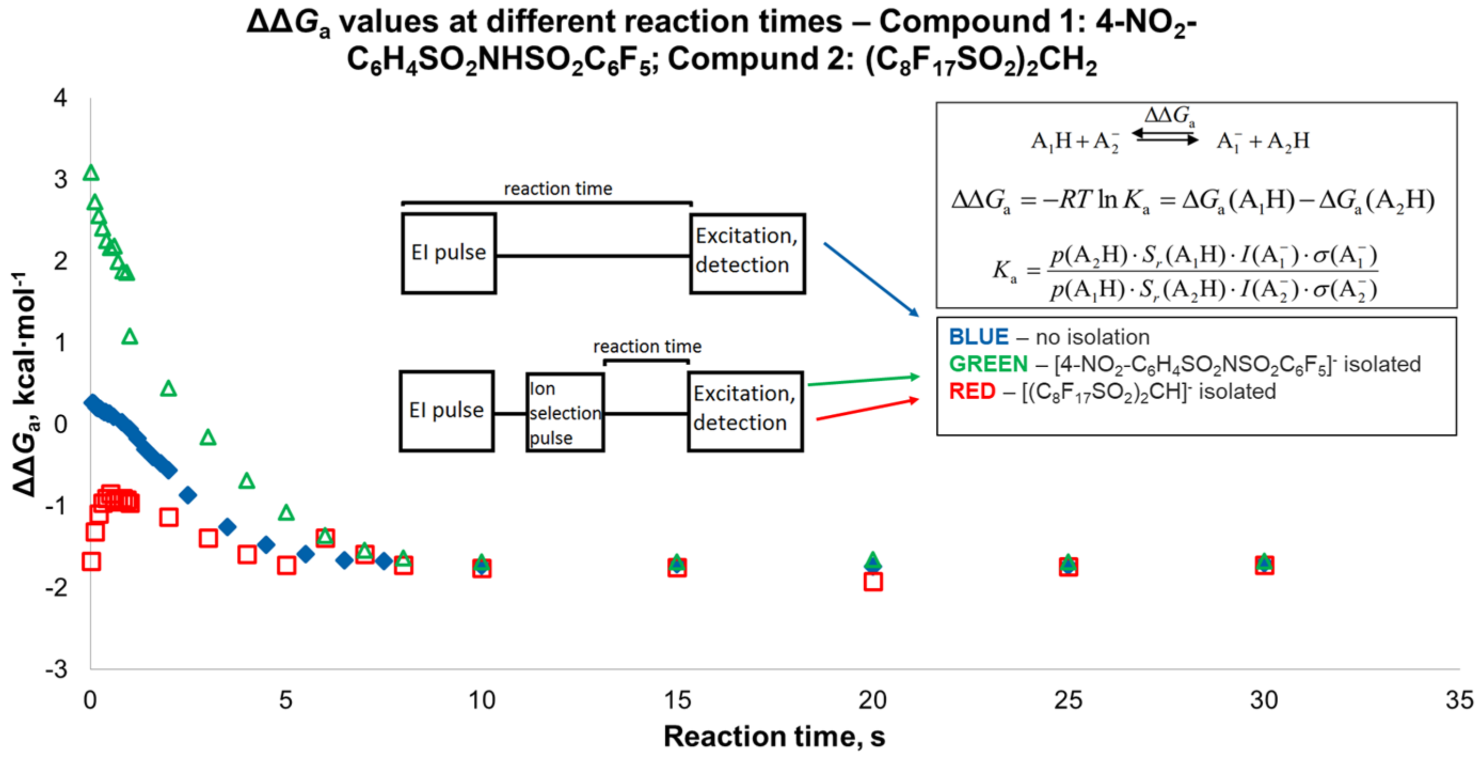

Figure 2. Example of the experimental data collected during a relative gas-phase acidity measurement, using the FT-ICR-MS equilibrium method, both with and without isolation of the conjugate base of one of the acids.

3.3 pK_a^{ow} measurement method

When measuring pK_a^{ow}, we monitor the dissociation reaction of the acid of interest in the octanol:water biphasic system with the phases being in equilibrium with each other. The directly measured quantity is the equilibrium constant (K_a^{ow}) of the dissociation reaction of this acid, denoted as HA, according to the following equilibrium (8):

$$\mathrm{HA_o} + \mathrm{Et_4N_w^+} \overset{K_a^{ow}}{\rightleftarrows} (\mathrm{A^-} \cdot \mathrm{Et_4N^+})_\mathrm{o} + \mathrm{H_w^+} \tag{8}$$

Subscripts “o” and “w” indicate the phase in which the species are mainly dissolved in. It is assumed that the rather lipophilic acid HA, as well as its conjugate base A^- mainly reside in the octanol phase. Due to the relatively low polarity of water-saturated octanol, A^- is predominantly in the form of an ion pair. Previous study on pK_a^{ow} values[14] shows that the composition of the aqueous phase, especially the ion that acts as a counter-ion in the acid-base equilibrium, can have a strong effect on the observed pK_a^{ow} values of the compounds. Based on tentative experiments performed in the current study, the pK_a^{ow} values of acids obtained with a more lipophilic counter-ion could be up to 3–4 pK_a units lower than the corresponding value obtained using a hydrophilic counter-ion, such as Na^+ or K^+. Et_4N^+ was used as the counter-ion used in this study. It is somewhere in the middle of this range as results with this counter-ion appear to be roughly 1 pK_a unit lower than with Na^+ or K^+. The main drawback to using a more hydrophilic counter-ion is that it leads to the compound of interest partitioning more into the aqueous phase as the stability of the ion pair in octanol phase is reduced. Often, these measurements operate at the lower limits of the concentration range in which the NMR measurement method is suitable. Due to this, use of hydrophilic counter-ions, and by extension, lower concentrations in the octanol phase, are generally undesirable.

As the properties and activity of the counter-cation strongly influence the ionization of the acid, the cation needs to be included in the standard state definition in order to ensure comparable results. In this study, tetraethylammonium (denoted as Et_4N^+) at concentration level 0.1 M was used. Et_4N^+ was chosen partly due to experimental considerations but also because there are various organic bases present in living organisms and Et_4N^+ could be a suitable approximation for their protonated forms.

Based on this, K_a^{ow} and pK_a^{ow} can be expressed by Eqs. 9–11. f_o denotes the ion pair’s activity coefficient in octanol. The activity of the neutral HA in octanol is assumed to be equal to its equilibrium concentration.

$$K_a^{ow} = \frac{a(\mathrm{H^+})_\mathrm{w} \cdot a(\mathrm{A^-} \cdot \mathrm{Et_4N^+})_\mathrm{o}}{a(\mathrm{HA})_\mathrm{o}} \tag{9}$$

$$\mathrm{p}K_a^{ow} = -\log K_a^{ow} = \mathrm{pH} - \log \frac{\cdot a(\mathrm{A^-} \cdot \mathrm{Et_4N^+})_\mathrm{o}}{a(\mathrm{HA})_\mathrm{o}} \tag{10}$$

$$\mathrm{p}K_{\mathrm{a}}^{\mathrm{ow}} = \mathrm{pH} - \log\frac{[\mathrm{A^-{\cdot}Et_4N^+}_{\mathrm{o}}]\cdot f_{\mathrm{o}}}{[\mathrm{HA_o}]} = \mathrm{pH} - \log\frac{[\mathrm{A^-{\cdot}Et_4N^+}_{\mathrm{o}}]}{[\mathrm{HA_o}]} - \log f_{\mathrm{o}} \qquad (11)$$

For each measurement, a roughly 1 mM solution of the compound of interest is prepared in stock octanol. If necessary, this solution is further diluted with octanol. For each sample, 2 mL of 1-octanol solution of the compound of interest was prepared into 4 mL vials and 2 mL of aqueous phase with measured pH was added. Aqueous phases with different pH values were generated by combining the following aqueous solutions in various ratios: (1) 0.1 M Et_4NCl + 0.01 M zwitterionic buffering agent HEPES; (2) 0.1 M HCl + 0.1 M Et_4NCl; (3) 0.1 M Et_4NOH. After preparation, the samples were equilibrated by shaking. Subsequently, the phases were separated by centrifuging the samples. Then, the pH of the samples was measured in the aqueous phase while the ratio of the equilibrium concentrations of the acid and its anion (conjugate base) at that pH was measured in the octanol phase, using one or both of NMR spectrometry and UV-Vis spectrometry.

From every measurement series an apparent $\mathrm{p}K_{\mathrm{a}}^{\mathrm{ow}}$ is calculated from the experimental data by using the least-squares method described in detail in publication II. In case of NMR measurements under fast proton exchange conditions, chemical shift values of the compound at different pH can be directly related to the ratio of the neutral acid and its conjugate base through degree of dissociation (α). Therefore, chemical shift values are plotted against the pH of the corresponding sample. A sigmoid curve is fitted to the data points so that the sum of squared distances on the chemical shift axis would be minimal. A similar approach was used for UV-Vis measurements (absorbance value at a chosen wavelength was used for the same purpose as chemical shift for NMR measurements). The apparent $\mathrm{p}K_{\mathrm{a}}^{\mathrm{ow}}$ value is one of the parameters varied in this least-squares optimization process.

The obtained apparent $\mathrm{p}K_{\mathrm{a}}^{\mathrm{ow}}$ values depend on the acid concentration they are measured at. Concentration-independent $\mathrm{p}K_{\mathrm{a}}^{\mathrm{ow}}$ values were calculated via extrapolation of the apparent $\mathrm{p}K_{\mathrm{a}}^{\mathrm{ow}}$ values to zero concentration using a Debye-Hückel-like model which is thoroughly explained in publication II. In case of relatively hydrophilic compounds, significant migration of the compound to the aqueous phase was frequently observed, resulting in lowered concentrations in the octanol phase. UV-Vis method was not suitable for the measurement of these compounds as the absorbance value depends on the concentration and the used method assumes constant concentration in the octanol phase. On the other hand, chemical shift is independent of the concentration and therefore, NMR method was used for compounds that exhibited significant partitioning into the aqueous phase. Reduction of concentration in the octanol phase, resulting from this partitioning, was taken into account by comparing peak areas (relative to a suitable octanol peak) of the sample with its pH closest to the $\mathrm{p}K_{\mathrm{a}}^{\mathrm{ow}}$ value and the sample with the lowest pH, corresponding to the sample where the acid was almost entirely in the neutral form. Reduced concentration was used as the estimate of the concentration at which the $\mathrm{p}K_{\mathrm{a}}^{\mathrm{ow}}$ value was measured. More details of this are given in Publication II.

4. RESULTS AND DISCUSSION

4.1 Gas-phase acidity measurements

4.1.1 Results of gas-phase acidity measurements

The section of the self-consistent gas-phase acidity scale measured in this work is presented in Table 1 and consists of 20 superacids. The consistency standard deviation of this section is 0.2 kcal·mol^{-1} indicating good consistency. In addition, the previous experimental literature values as well as acetonitrile and 1,2-dichloroethane acidity data are provided, where available. Each acid on the scale has been measured against at least two other compounds and there are multiple independent pathways from the top of the scale to the bottom, which enhances the reliability of the data.

Acid 20 extends the previously reported self-consistent experimental gas-phase acidity scale.

Table 1. Self-consistent gas-phase acidity scale compiled based on the results of this study

No.	Acid	Δ*GA*	*GA* exp.	*GA* lit.	MeCN pK_a	DCE[c] pK_a
1	$(CF_3SO_2)_2CH_2$	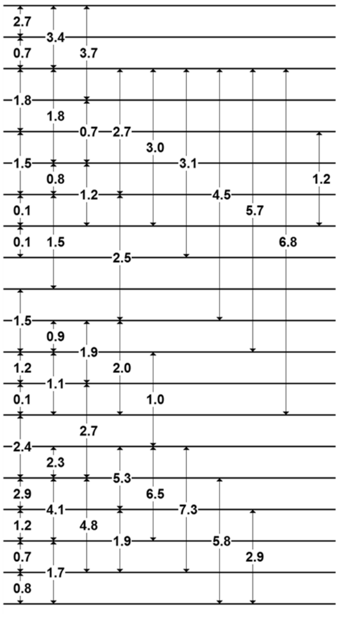	295.4	300.6[d]		
2	4-Cl-$C_6H_4SO_2NHSO_2C_6H_4$-4-NO_2		292.8	297.0[d]	9.17[e]	42.4[g]
3	**CF_3SO_3H**[b]		292.2	299.5[i]	0.70[f]	33.7[g]
4	$C_6F_5SO_2NHSO_2C_6H_4$-4-Cl		291.4	296.0[d]	7.57[e]	
5	3,5-$(NO_2)_2$-$C_6H_3SO_2NHSO_2C_6H_4$-4-CH_3		290.6			
6	$(C_3F_7SO_2)_2CH_2$		290.5			
7	$(C_4F_9SO_2)_2CH_2$		289.5	282.8[h]		
8	(3-NO_2-$C_6H_4SO_2)_2NH$		289.3	293.3[d]	8.15[d]	
9	2,4-$(NO_2)_2$-$C_6H_3SO_3H$		289.2		3.99[e]	36.0[g]
10	$(C_8F_{17}SO_2)_2CH_2$		288.0			
11	3-NO_2-$C_6H_4SO_2NHSO_2C_6H_3$-4-NO_2-3-Cl		287.4	291.1[d]	7.88[d]	
12	$C_6F_5SO_2NHSO_2C_6H_4$-4-NO_2		286.5	289.2[d]	6.60[e]	
13	$C_6F_5SO_2NHSO_2C_6H_3$-3-NO_2-4-Cl		285.4	287.8[d]	6.18[e]	
14	$(C_6F_5SO_2)_2NH$		285.3	287.5[d]	5.11[e]	
15	**$(FSO_2)_2NH$**[b]		285.3	283.1[h]		
16	$(CF_3SO_2)_2NH$		282.9	286.5[d]		33.0[g]
17	$(C_2F_5SO_2)_2NH$		280.0	283.9[h]	-0.10[f]	32.6[g]
18	$(C_3F_7SO_2)_2NH$		278.8	281.1[h]		32.7[g]
19	$(C_4F_9SO_2)_2NH$		278.0	278.7[h]		32.6[g]
20	$C_4F_9SO_2NHSO_2C_8F_{17}$		277.1			

[a] All *GA* values at 373K and in kcal mol^{-1}. GA exp. denotes values measured in this study while GA lit. denotes previously reported experimental values. [b] Results have been anchored to the computational *GA* values of acids **3** and **15** (W1BD, 291.3 and 286.2 kcal mol^{-1}, respectively). [c] 1,2-dichloroethane. [d] Ref [34]. [e] Ref [40]. [f] Ref [47]. [g] Ref [9]. [h] Ref [23]. [i] Ref [16].

As explained above, the directly measured quantities were the acidity differences (relative acidities), ΔGA values. Absolute *GA* values were assigned to the compounds in a two-step process. First, the initial *GA* values were assigned by minimizing the sum of squared differences between each of the measured ΔGA values with acids i and j, ΔGA_{ij}, and the difference in assigned *GA* values for the same pair of acids (GA_i and GA_j), as shown in Eq. 12.

$$\sum_{i,j}\left[\Delta GA_{ij} - (GA_i - GA_j)\right]^2 \rightarrow Min \tag{12}$$

In the second step, the obtained initial acidity scale was shifted in order to obtain the minimal possible differences between the independent *GA* values of the anchor compounds and their values on the scale. As discussed in Chapter 2.4, the choice of suitable anchor compounds in the range of gas-phase acidities investigated in this work is limited. Therefore, the scale is anchored to the computational *GA* values of triflic acid (291.3 kcal·mol^{-1}) and bis(fluorosulfonyl)imide (286.2 kcal·mol^{-1}), obtained using the high-level W1BD method (Publication I, computations were carried out by A. Trummal.). These are the only acids in the current study for which W1BD calculations were practical. The anchoring was done so that the *GA* values for triflic acid and bis(fluorosulfonyl)imide would be as close as possible to the computational values, while experimentally found differences in gas-phase acidity between these two acids, as well as other compounds studied, were maintained. Therefore, the values 292.2 and 285.3 kcal·mol^{-1} were assigned to triflic acid and bis(fluorosulfonyl)imide, respectively.

In all cases except for bis(nonafluorobutylsulfonyl)imide, there are significant discrepancies between the gas-phase acidities measured in this study and the previously reported values.[16,23,34] These differences are likely due to one or more of the following reasons:

1. **Anchoring.** As discussed in detail in Section 2.4, the previous experimental self-consistent gas-phase acidity scales involving superacids were anchored directly or indirectly to the *GA* value of HBr (318.28 kcal·mol^{-1} at 298.15 K).[1] This *GA* value is around 40 kcal·mol^{-1} higher than the gas-phase acidities of the most acidic compounds on the scale. Such range of gas-phase acidity is covered by tens of individual relative measurements. Therefore, anchoring the scale to HBr is likely to result in significant uncertainty in the strongest acid part of the scale. In this work, high-level computational *GA* values were used for anchoring.
2. **Method of choice for estimating partial pressures of the compounds.** The most common method used in previous studies for this purpose was the pressure gauge method,[16] which requires that changes in the total pressure of the high-vacuum system are caused only by changes in the partial pressures of the compounds being leaked into the high-vacuum system. During this study, it became clear that this requirement cannot always be satisfied. In this study, negative-ion short-reaction-time mass-spectra were used for estimating the partial pressure ratio of the acids. Details of this are provided in Publication I

3. **The presence of true equilibrium state was not explicitly verified in previous studies.** When using the relative FT-ICR-MS gas-phase acidity measurement method, equilibrium is considered to be reached when the equilibrium constants calculated at various reaction times form a plateau after a certain reaction time. However, such plateaus can sometimes be formed also before the true equilibrium state is reached, especially if the data points which form this plateau are collected over a relatively narrow range of reaction times. Under such circumstances, the ΔGA values observed may be vastly different from the ΔGA value observed in true equilibrium state. To avoid this, the data in this study were collected also in double resonance mode (Section 3.2). In case of true equilibrium state, the equilibrium constant observed in this mode is in agreement with the value obtained via the common approach. The presence of true equilibrium state was verified during each of the ΔGA measurements.

As a part of the current study, gas-phase acidities using G4(MP2) method were calculated for $(CF_3SO_2)_2CH_2$ and $(CF_3SO_2)_2NH$ (294.4 and 284.8 kcal·mol^{-1} at 373 K, respectively). The obtained experimental *GA* values are in satisfactory agreement with these values. This gives indirect evidence that the changes introduced to the measurement method and the current approach to anchoring the scale have led to improved reliability of the results obtained.

Notably, the current *GA* value for triflic acid 292.2 kcal mol^{-1} is in good to excellent agreement with previously reported computational data (290.2 kcal·mol^{-1},[5] 292.4 kcal·mol^{-1}[5]), unlike the previous experimentally reported values of 299.5 kcal·mol^{-1}[16] and 298.8 kcal·mol^{-1}.[15] Strictly speaking, the current value for triflic acid, presented in Table 1, cannot be considered experimental, as a computational *GA* value of triflic acid is used as one of the references. This was done to ensure the most accurate results possible. Using only bis(fluorosulfonyl)imide as a reference would shift all values in Table 1 upwards by 0.9 kcal·mol^{-1}, resulting in an experimental gas-phase acidity of 293.1 kcal·mol^{-1} for triflic acid, which would still be in a satisfactory agreement with the experimental data available when considering the uncertainties of the experimental and computational values themselves.

4.1.2 Relationships between structure and gas-phase acidity

The relationships found, based on the results of this study and the available MeCN and DCE acidity data, include the following:

1. The strength of $(C_xF_{2x+1}SO_2)_2CH_2$ and $(C_xF_{2x+1}SO_2)_2NH$ acids increases upon the increase of fluorocarbon chain length. (Fig. 3). However, the further the additional atoms are from the acidity center, the lower this increase is. The latter observation is especially pronounced in DCE,[9] as the 4 $(C_xF_{2x+1}SO_2)_2NH$ type acids, for which DCE acidity data is available, have relatively small differences in acidity in this solvent.

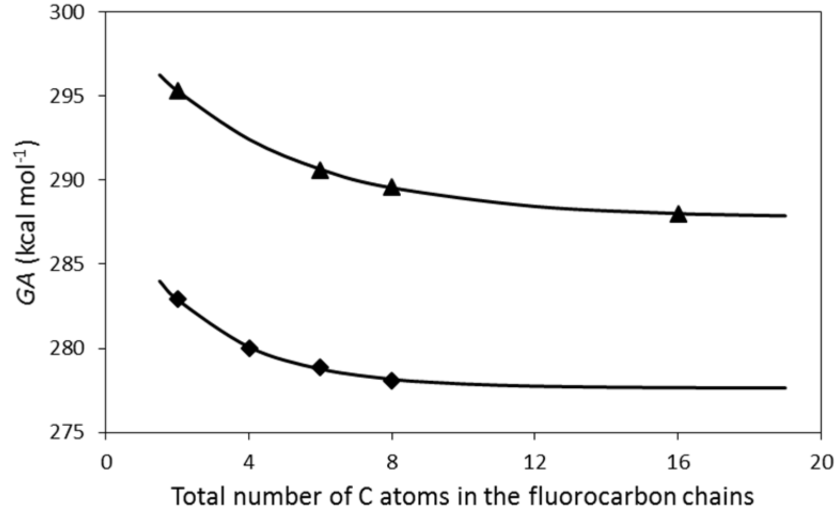

Figure 3. Experimental gas-phase acidities of the $(C_xF_{2x+1}SO_2)_2CH_2$ (▲) and $(C_xF_{2x+1}SO_2)_2NH$ (♦) acids with exponential decay functions as in ref. [48].

2. In general, the order of compounds in terms of acidity is similar in the gas phase and acetonitrile. The sulfonic acids included in this study are the most notable exceptions to this. 2,4-dinitrophenylsulfonic acid and, especially, triflic acid are relatively compact molecules in terms of structure. Anions derived from such acids (especially if they have spatially localized charges) often have higher solvation energies than bulkier anions with more pronounced charge delocalization[47] and therefore, relatively higher acidity in MeCN. In the gas-phase, solvation is absent and charge delocalization in an anion is generally a more important contributor to the stability of the conjugate base of the acid. Also, the efficiency of resonance stabilization is typically correlated with the size of the structure. Due to these factors, triflic acid and 2,4-dinitrobenzenesulfonic acid are weaker than $(C_6F_5SO_2)_2NH$ in the gas-phase by 4.3 and 2.3 pK_a units, respectively. On the other hand, in MeCN, triflic acid is stronger by 4.4 and 2,4-dinitrobenzenesulfonic acid by 1.1 pK_a units, compared to $(C_6F_5SO_2)_2NH$.
3. The increase in acidity upon introducing the $C_6F_5SO_2$– group appears to be more significant in MeCN than in the gas-phase. This effect is the most visible with $C_6F_5SO_2NHSO_2C_6H_3$-3-NO_2-4-Cl and $(C_6F_5SO_2)_2NH$. Their gas-phase acidities are very similar but in MeCN, the latter is stronger by more than 1 pK_a unit. Similar observation can be made when comparing the acidities of (3-NO_2-$C_6H_4SO_2)_2NH$ and $C_6F_5SO_2NHSO_2C_6H_4$-4-Cl. The former is more acidic in the gas-phase by 1.9 kcal·mol^{-1} or 1.1 pK_a units, while in MeCN the latter is more acidic by nearly 0.6 pK_a units.

4.1.3 Conclusions and outlook

Main conclusions drawn based on the gas-phase acidity measurements performed in this study:

- The changes introduced to the measurement and anchoring methods have likely led to appreciably increased reliability of the *GA* values obtained using the FT-ICR-MS equilibrium method for measuring gas-phase acidities.
- There is now sound agreement between the experimental and computational *GA* values of several acids featured also in the previous studies as *GA* values of these have been significantly (by up to 7.3 kcal mol^{-1}) revised.
- The aforementioned improvements serve as groundwork for expanding the gas-phase acidity scale even further.

Another result of this work was the extension of the self-consistent gas-phase acidity scale towards higher acidities (lower *GA* values). At a glance, extending the scale by just a single acid may not seem particularly impressive. However, these experiments also provided additional information about what kind of compounds would likely be needed to extend the scale further. Measurements were performed also with $(CF_3SO_2)_3CH$. Unfortunately, they were unsuccessful due to the apparently too large difference in acidity (> 4 kcal·mol^{-1}) between $(CF_3SO_2)_3CH$ and the strongest acid of the current scale $C_4F_9SO_2NHSO_2C_8F_{17}$. Nevertheless, this gap, based on both these experiments and available computational evidence,[5] appears to be likely within reach if compounds slightly more acidic than $C_4F_9SO_2NHSO_2C_8F_{17}$ or slightly less acidic than $(CF_3SO_2)_3CH$, such as $C_6F_5SO_2CH(SO_2CF_3)_2$, could be measured. Once this gap is bridged, it would likely open up a variety of options to extend the self-consistent gas-phase acidity scale significantly further, as the acidity of $(CF_3SO_2)_3CH$ type compounds can in theory be enhanced significantly by extending one or more of the fluorocarbon chains. It appears that the biggest obstacle to reaching new horizons in experimental gas-phase acidity is related to the difficulties with synthesis of suitable acids.

4.2 pK_a^{ow} measurements

4.2.1 Results of pK_a^{ow} measurements

In this study, pK_a^{ow} values of 37 uncharged acids were measured. The directly measured (apparent) pK_a^{ow} values depend on the concentration of the compound. Measurements were performed at various concentrations and the apparent pK_a^{ow} values were extrapolated to zero concentration, using the Debye-Hückel model.

The dependence on concentration is likely due to ionic strength effects on ion-ion interactions in the octanol phase. Therefore, to model this dependence, the second approximation of Debye-Hückel theory was used. The use of Debye-Hückel theory under the current experimental setup is a rather simplistic approach. However, it appears to describe this dependence surprisingly well, even though it was originally developed with the assumption of free ions, whereas the deprotonated acids are mainly present as ion pairs in octanol. The possibility of using the Debye-Hückel theory is likely due to the relatively weak Coulombic interactions between the anion and cation forming the ion pair and relatively strong interactions between the ion pair and the solvent.

The apparent pK_a^{ow} values (as a difference from the corresponding zero-concentration pK_a^{ow} values) along with the Debye-Hückel model fitted through all experimental points are shown on Fig. 4. The extrapolated values are presented in Table 2 with the available pK_a values in acetonitrile and water for comparison. Compounds of various structures and acidities are included. As can be seen from Fig. 4, there are no significant differences between the behavior of OH, NH and CH acids. Therefore, the use of the same Debye-Hückel model for all studied compounds is reasonable. The estimated standard uncertainty of the zero-concentration pK_a^{ow} values is 0.1 units.

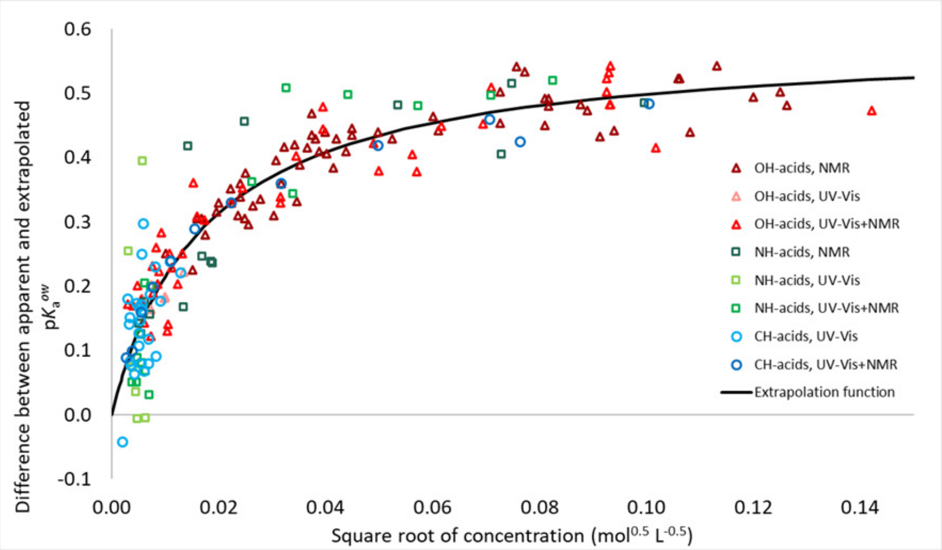

Figure 4. Overall representation of extrapolation of pK_a^{ow} values to zero concentration. Circles – CH acids, rectangles – NH acids, triangles – OH acids, solid line – the used Debye-Hückel model. Shades of data points indicate, which techniques were used (see the legend).

UV-Vis and NMR measurement methods were used. NMR measurements were performed using the following nuclei: ^{1}H, ^{13}C, ^{19}F and ^{31}P. The apparent pK_a^{ow} values obtained using different methods were in very good to excellent agreement (Publications II and III). The pros and cons of each measurement method used, their applicability and general practical considerations are discussed in Publications II and III.

The results show that the use of aqueous pK_a values for quantifying acid-base properties in biphasic systems consisting of an aqueous phase and a water-immiscible phase is not an adequate method. For example, based on aqueous pK_a values, most carboxylic acids are almost fully deprotonated at pH 7.4 which is the typical physiological pH. Many of them, especially the more lipophilic carboxylic acids, largely reside inside cell membranes (for which octanol is considered a decent approximation[45]) and fat tissue. In such environments, based on the results shown in Table 2, most of them would be mainly present as neutrals while it is often assumed from their aqueous pK_a values that they would be mainly deprotonated. Currently, pK_a^{ow} is probably the best available quantitative parameter of acid-base properties in such biphasic systems. This is because, unlike aqueous pK_a values which are often used for this purpose, pK_a^{ow} accounts for various processes, such as distribution and migration between phases, that take place in biphasic systems. The approach used in this study and its results are expected to be useful for researchers whose work involves biphasic systems.

Table 2. pK_a^{ow} values, extrapolated to zero concentration, of the acids measured in this study with available literature MeCN and H_2O acidities.

Compounds	**pK_a^{ow}**	**pK_a MeCN** [d]	**pK_a H_2O** [e]
Carboxylic acids			
sorbic acid	**7.7**[b]	**22.97**	**4.62**
cinnamic acid	**7.4**[b]		**4.44**
benzoic acid	**7.6**[b]	**21.5**	**4.20**
stearic acid	**8.0**[b]		
hexanoic acid	**8.0**[b]		**4.88**
lauric acid	**8.0**[b]		**4.85**
ibuprofen	**7.7**[b]		**4.31**
naproxen	**7.6**[b]		**4.18**
4-nitrobenzoic acid	**6.2**[b]	**19.9**[f]	**3.44**
2,4-dinitrobenzoic acid	**4.1**[b]	**16.6**[f]	**1.42**
1-pyrenecarboxylic acid	**7.1**[b,c]		
salicylic acid	**5.9**[b]	**16.7**	**2.99**
4-trifluoromethylbenzoic acid	**6.8**[b]		**3.67**
Other OH-acids			
Br_5-phenol	**7.0**[b,c]	**17.81**	**4.82**
Cl_5-phenol	**7.2**[c]	**18.00**	**4.75**
2,4,6-Br_3-phenol	**8.5**[b,c]	**20.34**	**6.17**
2-perfluoronaphthol	**7.0**[c]	**18.5**	
N-OH-phthalimide	**8.7**[b]		

Compounds	**pK_a^{ow}**	**pK_a MeCN** [d]	**pK_a H_2O** [e]
[Ph]-BPA-[H_8][h]	**2.3**[b]	**13.38**[g]	
diheptylphosphinic acid	**6.2**[b]		
NH-acids			
$3\text{-}NO_2\text{-}C_6H_4SO_2NHCOC_6H_4\text{-}3\text{-}Cl$	**4.2**[c]	**14.55**	
$4\text{-}NO_2\text{-}C_6H_4SO_2NHCOC_6H_4\text{-}3\text{-}Cl$	**4.0**[b,c]	**14.43**	
$4\text{-}NO_2\text{-}C_6H_4SO_2NHCOC_6H_4\text{-}3\text{-}OCH_3$	**4.6**[b,c]		
$4\text{-}NO_2\text{-}C_6H_4SO_2NHCOC_6H_4\text{-}4\text{-}CH_3$	**4.8** [b,c]	**15.68**	
$4\text{-}NO_2\text{-}C_6H_4SO_2NHCOC_6H_4\text{-}2\text{-}F$	**4.4** [b,c]		
$4\text{-}NO_2\text{-}C_6H_4\text{-}SO_2\text{-}NH_2$	**11.8** [b]	**24.57**	**9.04**
Tos_2NH [a]	**1.6** [b]	**11.97**	
Tos-NH-Boc [a]	**7.7** [b]		**5.05**
$(4\text{-}NC_5F_4)(C_6F_5)NH$	**11.6**[c]	**20.39**	
$(4\text{-}CN\text{-}C_6F_4)(C_6F_5)NH$	**11.6**[c]	**19.87**	
CH-acids			
$(4\text{-}NC_5F_4)(C_6F_5)CHCN$	**6.0**[c]	**16.39**	
$(4\text{-}NC_5F_4)(2\text{-}C_{10}F_7)CHCN$	**5.5**[c]	**16.01**	
$3\text{-}CF_3\text{-}C_6H_4CH(CN)_2$	**4.0**[b,c]	**14.70**	
$2\text{-}CN\text{-}C_6H_4CH(CN)_2$	**2.8**[c]		
$2,4\text{-}(CH_3O)_2\text{-}C_6H_3CH(CN)_2$	**9.1**[c]		
$(2\text{-}C_{10}F_7)CH(CN)COOEt$	**6.1**[c]	**17.48**	
$C_6F_5CH(CN)_2$	**2.2**[c]	**13.01**	

[a] Tos = $4\text{-}CH_3\text{-}C_6H_4\text{-}SO_2$-; Boc = *t*-BuOCO-. [b] Measured with NMR method. Nuclei used for the measurements with each compound are specified in Publications II and III. [c] Measured with UV-Vis method. [d] MeCN pK_a values from ref. [8], unless stated otherwise. [e] Aqueous pK_a values are from the [i] BonD databank http://ibond.nankai.edu.cn/ (references to original works are available in the SI of Publication II). [f] Values from refs. [42] and [49], corrected upwards by 0.8 and 0.4 pK_a units, respectively, to align with the values in ref [8]. [g] Estimated value, based on MeCN pK_a values of 9−[Phenanthrene]−BPA−[H8], [9−Phenanthrene]−BPA and [Ph]−BPA from ref. [8]. [h] Structure shown on Scheme S1 of Publication II.

4.2.2 Correlations of pK_a^{ow} with pK_a values in acetonitrile and water

pK_a^{ow} values were correlated with the available pK_a values in MeCN and H_2O. The following correlation equations (Eq. 13–14) were established (regression coefficients are given with standard deviations):

$$\mathrm{p}K_\mathrm{a}^\mathrm{ow} = (0.96 \pm 0.06) \cdot \mathrm{p}K_\mathrm{a}^{\mathrm{H_2O}} + (3.10 \pm 0.30);$$
$$n = 16, R^2 = 0.943, S = 0.38 \qquad (13)$$

$$\mathrm{p}K_\mathrm{a}^\mathrm{ow} = (0.76 \pm 0.09) \cdot \mathrm{p}K_\mathrm{a}^{\mathrm{MeCN}} - (7.19 \pm 1.69);$$
$$n = 22, R^2 = 0.766, \mathrm{S} = 1.43 \qquad (14)$$

Generally, in the case of Et_4N^+ counterion pK_a^{ow} values tend to be roughly 3 units higher and 11 units lower than corresponding aqueous and acetonitrile pK_a values, respectively. However, these differences are not constant. Correlation with aqueous pK_a values underestimates the pK_a^{ow} of ibuprofen and naproxen (by approximately 0.5 pK_a units), while the three halogenated phenols were the compounds with most overestimated pK_a^{ow} (by approximately 0.4 to 0.7 pK_a units). The differences between measured values and values predicted from correlations were for all compounds between -0.5 to 0.7 pK_a units. Importantly, in the correlation between pK_a^{ow} and aqueous pK_a values, there are no CH acids included because of the lack of aqueous pK_a values for the compounds involved. However, based on the aqueous pK_a values of some similar compounds in ref [47], it can be expected that the differences between pK_a^{ow} and aqueous pK_a values for the CH acids involved is smaller and might be below 2 pK_a units. The reason for this is likely that the more lipophilic anions of these compounds are less stabilized in water than the anions of OH and NH acids.

Correlation with MeCN acidities displays even higher scatter of points. It appears to significantly underestimate the pK_a^{ow} values of the two diphenylamines, by 3–4 pK_a units. Conversely, this correlation overestimates the pK_a^{ow} values of benzoic acid, 4-nitrobenzoic acid, 2,4-dinitrobenzoic acid and sorbic acid (by 1.4 to 2.7 units). For the other 12 compounds for which MeCN pK_a is available, the differences between correlated and measured pK_a^{ow} values were between -0.6 to 0.8 units.

These differences demonstrate that there are nuances to the acid-base properties in biphasic systems that cannot be estimated from “monophasic” pK_a values via simple correlation analysis.

4.2.3 Conclusions and outlook

Main conclusions drawn from the pK_a^{ow} measurements performed in this study:

- Measured pK_a^{ow} values differ significantly (by several units) from the corresponding aqueous pK_a values, further highlighting the fact that aqueous (or any other monophasic) pK_a values are not suitable for quantitatively estimating acidity in biphasic systems such as cell membranes.
- The current study significantly expands the number of compounds for which pK_a^{ow} values are available. A number of well-known acids, such as benzoic acid, salicylic acid and ibuprofen, were measured in this study.
- The NMR measurement method developed in this study significantly expands the choice of compounds for which pK_a^{ow} can be measured. All 4 of

the nuclei used in this study (^{1}H, ^{13}C, ^{19}F, ^{31}P) are suitable for these measurements as they yielded consistent results.
- Biphasic acidity as a concept requires further investigation.

pK_a^{ow} is a relatively novel concept as previous research on pK_a^{ow} values is limited to only a few rather exotic bases. The most important aspect of these measurements is the relevance of the results to practical situations. One potential application of pK_a^{ow} could be biological systems. For example, octanol is considered a relatively good approximation for lipid membranes,[45] although the membrane itself consists of a large number of different compounds.[50] Similarly, there is a wide variety of ions in both intracellular fluid and extracellular fluid. It is likely that there are counter-ions which would be more suitable to approximate the ion-pair stabilizing effect in cell membranes and other biological biphasic systems than the currently used Et_4N^+ ion. Identifying these ions could help further develop the pK_a^{ow} concept towards more relevant results.

The current study on pK_a^{ow} involves a variety of acids of various structures and properties, different experimental approaches and considerations are discussed in detail. Many of the findings from this study are likely to be relevant for bases as well. However, as the previous research on pK_a^{ow} values of bases is limited to the initial study which included just a few rather exotic iminophosphorane bases, a more comprehensive study, encompassing the common organic bases, is needed for bases.

A further exciting development avenue of biphasic pK_a measurements could be the ability to perform these measurements directly in cell membranes. This would require nano-scale measurement of both NMR spectra and pH. Versions of similar applications have been suggested and designed.[51,52] The suitability of these or any other similar applications for measuring specifically the biphasic pK_a of a compound in a cell membrane is difficult to assess without an in-depth study designed for this purpose.

SUMMARY

In this study, two problematic areas of Brønsted acidity that require further research were identified and investigated.

One of these is gas-phase acidity. Gas-phase acidities of compounds represent a measure of their Brønsted acidity without solvent effects. Therefore, knowing gas-phase acidities of compounds helps us better understand solvent effects as well as substituent effects in both gas phase and solvents. Furthermore, gas-phase acidities are useful for the development and testing of computational methods as the dissociation reaction of an acid in the gas-phase is usually simple in its nature and the range of acidities that can be observed in the gas-phase is practically limitless. The gas-phase acidity scale in the range of very weak to medium-strong acids has been reliably established. However, before this work, the same could not be said about the superacidic part of the gas-phase acidity scale. The reliability of the experimental gas-phase acidities reported for many important superacids, such as triflic acid, had been called into question. In addition, computational studies show that gas-phase acidity scale can be extended significantly further towards higher acidities. In order to address these issues, changes were introduced to the previous FT-ICR-MS method for measuring relative gas-phase acidities. Based on measurements with the improved method, a self-consistent segment of the gas-phase acidity scale consisting of 20 superacids, including triflic acid, and ranging from 295.4 to 277.1 kcal mol^{-1} i.e., around 13 orders of magnitude. The scale was anchored using gas-phase acidities obtained from a high-level computational method (W1BD) as there are no suitable reference compounds in the sub-300 kcal·mol^{-1} range known to us for which the absolute gas-phase acidity has been measured with sufficient reliability. The current study extends the previous self-consistent gas-phase acidity scale towards higher acidities. The results exhibit significantly improved consistency and agreement with available computational data and can therefore be considered reliable.

The other topic of focus was biphasic acidity. Biphasic systems are present in a variety of applications and in all living organisms. However, acidity of ligands, catalysts and other compounds with important roles in these systems are almost universally estimated from single-phase pK_a values. This cannot be considered a reliable approach as biphasic systems involve additional processes, such as distribution between phases or ion-pairing, that in a single-phase system are simpler in their nature or not present at all, such as phase transfer. Recently, the concept of biphasic acidity was developed and as the first measurements in an octanol:water system with protonated acids have shown, these biphasic pK_a (pK_a^{ow}) values are significantly different from the corresponding aqueous pK_a values which are typically used for estimating acidity in biphasic systems consisting of an aqueous phase at equilibrium with a water-immiscible phase. Before this work, there were no pK_a^{ow} values available for neutral acids. In this study, the previous UV-Vis measurement method was slightly improved and an

NMR method (used with 4 different nuclei) for measuring pK_a^{ow} was developed. Using these methods, pK_a^{ow} values were measured for 37 neutral acids, including such important compounds, as ibuprofen, benzoic acid and sorbic acid. The methods as well as their advantages and disadvantages were thoroughly discussed. However, there are other aspects of pK_a^{ow} values that need to be further studied.

REFERENCES

[1] K. M. Ervin, V. F. DeTuri, *J. Phys. Chem. A* **2002**, *106*, 9947–9956.

[2] C. H. DePuy, S. Gronert, S. E. Barlow, V. M. Bierbaum, R. Damrauer, *J. Am. Chem. Soc.* **1989**, *111*, 1968–1973.

[3] L. Lipping, I. Leito, I. Koppel, I. Krossing, D. Himmel, I. A. Koppel, *J. Phys. Chem. A* **2015**, *119*, 735–743.

[4] L. Lipping, I. Leito, I. Koppel, I. A. Koppel, *J. Phys. Chem. A* **2009**, *113*, 12972–12978.

[5] K. E. Gutowski, D. A. Dixon, *J. Phys. Chem. A* **2006**, *110*, 12044–12054.

[6] V. Palm, *Tables of Rate and Equilibrium Constants of Heterolytic Organic Reactions*, VINITI, Moscow-Tartu, **1975**.

[7] F. G. Bordwell, *Acc. Chem. Res.* **1988**, *21*, 456–463.

[8] A. Kütt, S. Tshepelevitsh, J. Saame, M. Lõkov, I. Kaljurand, S. Selberg, I. Leito, *Eur. J. Org. Chem.* **2021**, *2021*, 1407–1419.

[9] E. Paenurk, K. Kaupmees, D. Himmel, A. Kütt, I. Kaljurand, I. A. Koppel, I. Krossing, I. Leito, *Chem. Sci.* **2017**, *8*, 6964–6973.

[10] K. Izutsu, *Acid-Base Dissociation Constants in Dipolar Aprotic Solvents*, Blackwell Scientific Publications ; Distributors, USA, Publishers’ Business Services, Oxford ; Boston : Brookline Village, Mass, **1990**.

[11] L. M. J. Sprakel, B. Schuur, *Sep. Purif. Technol.* **2019**, *211*, 935–957.

[12] L. Zong, C.-H. Tan, *Acc. Chem. Res.* **2017**, *50*, 842–856.

[13] X. Pei, D. Xiong, H. Wang, S. Gao, X. Zhang, S. Zhang, J. Wang, *Angew. Chem.* **2018**, *130*, 3749–3753.

[14] S. Selberg, S. Tshepelevitsh, I. Leito, *Croat. Chem. Acta* **2018**, *91*.

[15] A. A. Viggiano, M. J. Henchman, F. Dale, C. A. Deakyne, J. F. Paulson, *J. Am. Chem. Soc.* **1992**, *114*, 4299–4306.

[16] I. A. Koppel, R. W. Taft, F. Anvia, S.-Z. Zhu, L.-Q. Hu, K.-S. Sung, D. D. DesMarteau, L. M. Yagupolskii, Y. L. Yagupolskii, *J. Am. Chem. Soc.* **1994**, *116*, 3047–3057.

[17] D. Himmel, S. K. Goll, I. Leito, I. Krossing, *Chem. - Eur. J.* **2012**, *18*, 9333–9340.

[18] A. Kütt, I. Leito, I. Kaljurand, L. Sooväli, V. M. Vlasov, L. M. Yagupolskii, I. A. Koppel, *J. Org. Chem.* **2006**, *71*, 2829–2838.

[19] R. W. Taft, F. G. Bordwell, *Acc. Chem. Res.* **1988**, *21*, 463–469.

[20] A. Kütt, V. Movchun, T. Rodima, T. Dansauer, E. B. Rusanov, I. Leito, I. Kaljurand, J. Koppel, V. Pihl, I. Koppel, G. Ovsjannikov, L. Toom, M. Mishima, M. Medebielle, E. Lork, G.-V. Röschenthaler, I. A. Koppel, A. A. Kolomeitsev, *J. Org. Chem.* **2008**, *73*, 2607–2620.

[21] P. Burk, I. A. Koppel, I. Koppel, I. Leito, O. Travnikova, *Chem. Phys. Lett.* **2000**, *323*, 482–489.

[22] M. M. Meyer, X.-B. Wang, C. A. Reed, L.-S. Wang, S. R. Kass, *J. Am. Chem. Soc.* **2009**, *131*, 18050–18051.

[23] M. Zhang, T. Sonoda, M. Mishima, T. Honda, I. Leito, I. A. Koppel, W. Bonrath, T. Netscher, *J. Phys. Org. Chem.* **2014**, *27*, 676–679.

[24] N. F. Hall, J. B. Conant, *J. Am. Chem. Soc.* **1927**, *49*, 3047–3061.

[25] G. A. Olah, *Superacid Chemistry*, Wiley, Hoboken, N.J., **2009**.

[26] R. D. Howells, J. D. McCown, *Chem. Rev.* **1977**, *77*, 69–92.

[27] G. A. Olah, G. K. S. Prakash, J. Sommer, *Science* **1979**, *206*, 13–20.

[28] I. Krossing, I. Raabe, *Angew. Chem. Int. Ed.* **2004**, *43*, 2066–2090.

[29] P. Bonhôte, A.-P. Dias, N. Papageorgiou, K. Kalyanasundaram, M. Grätzel, *Inorg. Chem.* **1996**, *35*, 1168–1178.

[30] M. Hayyan, F. S. Mjalli, M. A. Hashim, I. M. AlNashef, T. X. Mei, *J. Ind. Eng. Chem.* **2013**, *19*, 106–112.

[31] D. D. DesMarteau, *Science* **2000**, *289*, 72–73.

[32] N. Nishi, T. Uruga, H. Tanida, T. Kakiuchi, *Langmuir* **2011**, *27*, 7531–7536.

[33] A. Noda, K. Hayamizu, M. Watanabe, *J. Phys. Chem. B* **2001**, *105*, 4603–4610.

[34] I. Leito, E. Raamat, A. Kütt, J. Saame, K. Kipper, I. A. Koppel, I. Koppel, M. Zhang, M. Mishima, L. M. Yagupolskii, R. Yu. Garlyauskayte, A. A. Filatov, *J. Phys. Chem. A* **2009**, *113*, 8421–8424.

[35] A. Trummal, L. Lipping, I. Kaljurand, I. A. Koppel, I. Leito, *J. Phys. Chem. A* **2016**, *120*, 3663–3669.

[36] E. C. Barnes, G. A. Petersson, J. A. Montgomery, M. J. Frisch, J. M. L. Martin, *J. Chem. Theory Comput.* **2009**, *5*, 2687–2693.

[37] S. Rayne, K. Forest, *J. Chem. Eng. Data* **2010**, *55*, 5359–5364.

[38] I. Koppel, J. Koppel, P.-C. Maria, J.-F. Gal, R. Notario, V. M. Vlasov, R. W. Taft, *Int. J. Mass Spectrom. Ion Process.* **1998**, *175*, 61–69.

[39] J. Reijenga, A. van Hoof, A. van Loon, B. Teunissen, *Anal. Chem. Insights* **2013**, *8*, ACI.S12304.

[40] A. Kütt, T. Rodima, J. Saame, E. Raamat, V. Mäemets, I. Kaljurand, I. A. Koppel, R. Yu. Garlyauskayte, Y. L. Yagupolskii, L. M. Yagupolskii, E. Bernhardt, H. Willner, I. Leito, *J. Org. Chem.* **2011**, *76*, 391–395.

[41] W. S. Matthews, J. E. Bares, J. E. Bartmess, F. G. Bordwell, F. J. Cornforth, G. E. Drucker, Z. Margolin, R. J. McCallum, G. J. McCollum, N. R. Vanier, *J. Am. Chem. Soc.* **1975**, *97*, 7006–7014.

[42] I. M. Kolthoff, M. K. Chantooni, *J. Phys. Chem.* **1966**, *70*, 856–866.

[43] E. Parman, L. Toom, S. Selberg, I. Leito, *J. Phys. Org. Chem.* **2019**, *32*, e3940.

[44] D. Himmel, S. K. Goll, I. Leito, I. Krossing, *Angew. Chem. Int. Ed.* **2010**, *49*, 6885–6888.

[45] R. N. Smith, C. Hansch, M. M. Ames, *J. Pharm. Sci.* **1975**, *64*, 599–606.

[46] I. Kaljurand, J. Saame, T. Rodima, I. Koppel, I. A. Koppel, J. F. Kögel, J. Sundermeyer, U. Köhn, M. P. Coles, I. Leito, *J. Phys. Chem. A* **2016**, *120*, 2591–2604.

[47] E. Raamat, K. Kaupmees, G. Ovsjannikov, A. Trummal, A. Kütt, J. Saame, I. Koppel, I. Kaljurand, L. Lipping, T. Rodima, V. Pihl, I. A. Koppel, I. Leito, *J. Phys. Org. Chem.* **2013**, *26*, 162–170.

[48] I. Leito, I. A. Koppel, I. Koppel, K. Kaupmees, S. Tshepelevitsh, J. Saame, *Angew. Chem. Int. Ed.* **2015**, *54*, 9262–9265.

[49] I. M. Kolthoff, M. K. Chantooni, *J. Am. Chem. Soc.* **1970**, *92*, 7025–7030.

[50] J. L. Tymoczko, J. M. Berg, L. Stryer, *Biochemistry, a Short Course*, W.H. Freeman & Company, A Macmillan Education Imprint, New York, **2015**.

[51] I. Schwartz, J. Rosskopf, S. Schmitt, B. Tratzmiller, Q. Chen, L. P. McGuinness, F. Jelezko, M. B. Plenio, *Sci. Rep.* **2019**, *9*, 6938.

[52] S. W. Bishnoi, C. J. Rozell, C. S. Levin, M. K. Gheith, B. R. Johnson, D. H. Johnson, N. J. Halas, *Nano Lett.* **2006**, *6*, 1687–1692.

SUMMARY IN ESTONIAN

Kvantitatiivsed Brønstedi happelisuse mõõtmised kahefaasilistes süsteemides ning gaasifaasis

Käesolev doktoritöö põhineb kahel Brønstedi happelisuse rakendusel, mille puhul leiti, et nendega seotud varasemas teadustöös esinevad tõsised puudused.

Üks nendest rakendustest on gaasifaasiline happelisus. Ühendite gaasifaasiline happelisus väljendab nende lahustist sõltumatut happelisust. Gaasifaasiliste happelisuste teadmine aitab paremini mõista solvendiefekte ja substituendiefekte nii gaasifaasis kui ka vedelikes. Gaasifaasiline happelisus on sobilik arvutuslike meetodite väljatöötamiseks ja testimiseks, sest happe dissotsiatsioonireaktsioon gaasifaasis on oma olemuselt lihtsakoeline ning uuritavate happelisuste vahemik gaasifaasis on sisuliselt piiramatu. Nõrkade kuni mõõdukalt tugevate hapete jaoks on gaasifaasilise happelisuse skaala usaldusväärselt paigas. Seevastu superhapete gaasifaasiliste happelisuste osas esines enne käesolevat tööd märgatav ebakindlus. Mitmete oluliste superhapete, nagu näiteks trifluorometaansulfoonhappe, jaoks mõõdetud gaasifaasilise happelisuse väärtusi peeti kaheldavaks. Samuti viitavad mitmed arvutuslikele meetoditele põhinevad tööd, et gaasifaasilise happelisuse skaala on ulatuslikult laiendatav kasvava happelisuse suunas.

Selleks, et püüda eelpool toodud probleeme lahendada, täiustati käesolevas töös varasemat FT-ICR-MS meetodit gaasifaasiliste happelisuste mõõtmiseks suhtelise mõõtmismetoodika alusel. Täiustatud meetodit rakendati 20 superhappe gaasifaasiliste happelisuste mõõtmiseks. Tulemuste põhjal koostati kooskõlalise gaasifaasilise happelisuse skaala lõik vahemikus 295.4 kuni 277.1 kcal mol^{-1}, selline vahemik vastab ligikaudu 13 pK_a ühikule. Skaala ankurdamiseks kasutati kõrgetasemelise kvantkeemilise arvutusmeetodi, W1BD, abil saadud gaasifaasilisi happelisusi, sest sobivaid referentsühendeid gaasifaasilise happelisusega alla 300 kcal mol^{-1} teadaolevalt ei esine. Käesoleva töö tulemused pikendavad varasemat gaasifaasilise happelisuse skaalat ning on heas kooskõlas omavahel, samuti on selle töö tulemused varasematega võrreldes oluliselt paremas kooskõlas saadaolevate arvutuslike andmetega. Sellest lähtuvalt võib käesoleva töös mõõdetud gaasifaasilisi happelisusi pidada usaldusväärseteks.

Doktoritöö teiseks teemaks on kahefaasilised happelisused. Kahefaasilised süsteemid esinevad mitmesugustes rakendustes ning ka kõigis elusorganismides. Samas, erinevate ligandide, katalüsaatorite ja teiste oluliste molekulide happelisuste kvantitatiivse hinnanguga kasutatakse peaaegu alati ühefaasilist pK_a väärtust. Selline lähenemine ei ole põhjendatud, sest kahefaasilised süsteemid hõlmavad lisaks dissotsiatsioonile faasiülekandeprotsesse, mida ühefaasilistes süsteemides ei esine, aga mis oluliselt mõjutavad hapete käitumist. Hiljuti töötati välja kahefaasilise happelisuse kontseptsioon. Esimesed sellel põhinevad mõõtmised oktanool:vesi süsteemis näitavad, et ühendite kahefaasiline happelisus (väljendatuna kahefaasilise pK_a ehk pK_a^{ow} väärtusena) erinevad tunduvalt vastava ühendi vesilahuse $\mathrm{p}K_\mathrm{a}$ väärtusest. Süsteemides, kus veefaas on tasakaalus vees mittelahustuva faasiga, kasutatakse peamiselt aga just vesilahuse $\mathrm{p}K_\mathrm{a}$ väärtusi ühendite happelisuse kvantitatiivse hinnanguna. Neutraalsetele hapetele pole varasemalt $\mathrm{p}K_\mathrm{a}^\mathrm{ow}$ väärtusi mõõdetud. Käesolevas töös täiustati põgusalt varasemat UV-Vis spektroskoopial põhinevat $\mathrm{p}K_\mathrm{a}^\mathrm{ow}$ mõõtmismeetodit ning töötati välja tuumamagnetresonantsspektroskoopial põhinev mõõtmismeetod (4 erineva tuumaga). Nende meetodite abil mõõdeti 37 erineva neutraalse happe, sealhulgas selliste oluliste ainete, nagu ibuprofeeni, bensoehappe ja sorbiinhappe, $\mathrm{p}K_\mathrm{a}^\mathrm{ow}$ väärtused. Kasutatud meetodeid ning nende eeliseid ja puuduseid kirjeldati põhjalikult. Samas, mitmeid erinevaid $\mathrm{p}K_\mathrm{a}^\mathrm{ow}$ väärtustega seotud aspekte on vajalik täiendavalt uurida.

ACKNOWLEDGEMENTS

I am extremely grateful to Professor Ivo Leito for his leadership, guidance, patience, trust and in general, time he has invested into me and my scientific work through all these years and all my academic degrees.

I am also grateful to Ivari Kaljurand for teaching me the basics as well as the specifics of the FT-ICR-MS instrument at University of Tartu. I thank Sigrid Selberg for her help with the biphasic pK_a measurements and Lauri Toom for his help with NMR measurements as well as relevant insight.

I appreciate Tõiv Haljasorg for all the chemistry-related discussions through the years, the very first lessons regarding practical work and last but not least, making my wedding a truly unforgettable experience.

I am grateful to my wife, Agnieszka, for her unwavering support for everything related to the University of Tartu.

I am thankful to all of my colleagues at the chair Analytical Chemistry and other contributors and collaborators both in Estonia and abroad. Most of them have not been personally singled out here, yet their help and friendship has been crucial as well.

This research was funded from the EMPIR programme (project 17FUN09 “UnipHied”, www.uniphied.eu) co-financed by the Participating States and from the European Union’s Horizon 2020 research and innovation programme, by the Estonian Research Council grants (PRG690) and by EU through the European Regional Development Fund under project TK141 “Advanced materials and high-technology devices for energy recuperation systems” (2014-2020. 4.01.15-0011). This work was carried out using the instrumentation at the Estonian Center of Analytical Chemistry (www.akki.ee).

PUBLICATIONS

CURRICULUM VITAE

Name: Andre Leesment
Date of birth: December 11, 1991, Tartu
Citizenship: Estonia
E-mail: andre.leesment@ut.ee

EDUCATION:

2018–…	University of Tartu, Institute of Chemistry, PhD student
2016–2018	University of Tartu, Institute of Chemistry, MSc, *cum laude* (Chemistry)
2013–2016	University of Tartu, Institute of Chemistry, BSc, *cum laude* (Chemistry)

PROFESSIONAL EMPLOYMENT

2020–…	University of Tartu, Institute of Chemistry, Chemist

SCIENTIFIC PUBLICATIONS

1. A. Leesment, I. Kaljurand, A. Trummal, A. Kütt, T. Netscher, W. Bonrath, I. Leito, “Validation and extension of the gas-phase superacidity scale”. *Rapid Commun. Mass Spectrom.* **2020**, *e8598*.
2. A. Leesment, S. Selberg, M. Tammiste, A. H. Vu, T. H. Nguyen, L. Taylor-King, I. Leito, “Quantifying Acidity in Heterogeneous Systems: Biphasic pK_a Values”. *Anal. Chem.* **2022**, *94*, 4059–4064
3. A. Leesment, S. Selberg, I. Leito, “NMR as biphasic pK_a measurement technique”. *J. Chem. Metrol.* **2023**, *2*, 60–67.

REPORTS ON CONFERENCES

1. A. Leesment, I. Leito, I. Kaljurand “Validation of Gas-Phase Acidity Measurements of Superacids”. Eurachem 2019, Estonia, Tartu (20–24.05.2019). Poster presentation.

ELULOOKIRJELDUS

Nimi	Andre Leesment
Sünniaeg	11. detsember 1991, Tartu
Kodakondsus	eesti
E-mail	andre.leesment@ut.ee

HARIDUSKÄIK

2018–…	Tartu Ülikool, *keemia eriala doktoriõpe*
2016–2018	Tartu Ülikool, MSc, keemia
2013–2016	Tartu Ülikool, BSc, keemia

TÖÖKOGEMUS

2020–…	Tartu Ülikool, keemik

TEADUSPUBLIKATSIOONID

1. A. Leesment, I. Kaljurand, A. Trummal, A. Kütt, T. Netscher, W. Bonrath, I. Leito, “Validation and extension of the gas-phase superacidity scale”. *Rapid Commun. Mass Spectrom.* **2020**, *e8598*.
2. A. Leesment, S. Selberg, M. Tammiste, A. H. Vu, T. H. Nguyen, L. Taylor-King, I. Leito, “Quantifying Acidity in Heterogeneous Systems: Biphasic pK_a Values”. *Anal. Chem.* **2022**, *94*, 4059–4064
3. A. Leesment, S. Selberg, I. Leito, “NMR as biphasic pK_a measurement technique”. *J. Chem. Metrol.* **2023**, *2*, 60–67.

KONVERENTSID

1. A. Leesment, I. Leito, I. Kaljurand “Validation of Gas-Phase Acidity Measurements of Superacids”. Eurachem 2019, Estonia, Tartu (20–24.05.2019). Stendiettekanne.

DISSERTATIONES CHIMICAE
UNIVERSITATIS TARTUENSIS

1. **Toomas Tamm.** Quantum-chemical simulation of solvent effects. Tartu, 1993, 110 p.
2. **Peeter Burk.** Theoretical study of gas-phase acid-base equilibria. Tartu, 1994, 96 p.
3. **Victor Lobanov.** Quantitative structure-property relationships in large descriptor spaces. Tartu, 1995, 135 p.
4. **Vahur Mäemets.** The ^{17}O and ^{1}H nuclear magnetic resonance study of H_2O in individual solvents and its charged clusters in aqueous solutions of electrolytes. Tartu, 1997, 140 p.
5. **Andrus Metsala.** Microcanonical rate constant in nonequilibrium distribution of vibrational energy and in restricted intramolecular vibrational energy redistribution on the basis of slater's theory of unimolecular reactions. Tartu, 1997, 150 p.
6. **Uko Maran.** Quantum-mechanical study of potential energy surfaces in different environments. Tartu, 1997, 137 p.
7. **Alar Jänes.** Adsorption of organic compounds on antimony, bismuth and cadmium electrodes. Tartu, 1998, 219 p.
8. **Kaido Tammeveski.** Oxygen electroreduction on thin platinum films and the electrochemical detection of superoxide anion. Tartu, 1998, 139 p.
9. **Ivo Leito.** Studies of Brønsted acid-base equilibria in water and non-aqueous media. Tartu, 1998, 101 p.
10. **Jaan Leis.** Conformational dynamics and equilibria in amides. Tartu, 1998, 131 p.
11. **Toonika Rinken.** The modelling of amperometric biosensors based on oxidoreductases. Tartu, 2000, 108 p.
12. **Dmitri Panov.** Partially solvated Grignard reagents. Tartu, 2000, 64 p.
13. **Kaja Orupõld.** Treatment and analysis of phenolic wastewater with microorganisms. Tartu, 2000, 123 p.
14. **Jüri Ivask.** Ion Chromatographic determination of major anions and cations in polar ice core. Tartu, 2000, 85 p.
15. **Lauri Vares.** Stereoselective Synthesis of Tetrahydrofuran and Tetrahydropyran Derivatives by Use of Asymmetric Horner-Wadsworth-Emmons and Ring Closure Reactions. Tartu, 2000, 184 p.
16. **Martin Lepiku.** Kinetic aspects of dopamine D_2 receptor interactions with specific ligands. Tartu, 2000, 81 p.
17. **Katrin Sak.** Some aspects of ligand specificity of P2Y receptors. Tartu, 2000, 106 p.
18. **Vello Pällin.** The role of solvation in the formation of iotsitch complexes. Tartu, 2001, 95 p.
19. **Katrin Kollist.** Interactions between polycyclic aromatic compounds and humic substances. Tartu, 2001, 93 p.

20. **Ivar Koppel.** Quantum chemical study of acidity of strong and superstrong Brønsted acids. Tartu, 2001, 104 p.
21. **Viljar Pihl.** The study of the substituent and solvent effects on the acidity of OH and CH acids. Tartu, 2001, 132 p.
22. **Natalia Palm.** Specification of the minimum, sufficient and significant set of descriptors for general description of solvent effects. Tartu, 2001, 134 p.
23. **Sulev Sild.** QSPR/QSAR approaches for complex molecular systems. Tartu, 2001, 134 p.
24. **Ruslan Petrukhin.** Industrial applications of the quantitative structure-property relationships. Tartu, 2001, 162 p.
25. **Boris V. Rogovoy.** Synthesis of (benzotriazolyl)carboximidamides and their application in relations with *N*- and *S*-nucleophyles. Tartu, 2002, 84 p.
26. **Koit Herodes.** Solvent effects on UV-vis absorption spectra of some solvatochromic substances in binary solvent mixtures: the preferential solvation model. Tartu, 2002, 102 p.
27. **Anti Perkson.** Synthesis and characterisation of nanostructured carbon. Tartu, 2002, 152 p.
28. **Ivari Kaljurand.** Self-consistent acidity scales of neutral and cationic Brønsted acids in acetonitrile and tetrahydrofuran. Tartu, 2003, 108 p.
29. **Karmen Lust.** Adsorption of anions on bismuth single crystal electrodes. Tartu, 2003, 128 p.
30. **Mare Piirsalu.** Substituent, temperature and solvent effects on the alkaline hydrolysis of substituted phenyl and alkyl esters of benzoic acid. Tartu, 2003, 156 p.
31. **Meeri Sassian.** Reactions of partially solvated Grignard reagents. Tartu, 2003, 78 p.
32. **Tarmo Tamm.** Quantum chemical modelling of polypyrrole. Tartu, 2003. 100 p.
33. **Erik Teinemaa.** The environmental fate of the particulate matter and organic pollutants from an oil shale power plant. Tartu, 2003. 102 p.
34. **Jaana Tammiku-Taul.** Quantum chemical study of the properties of Grignard reagents. Tartu, 2003. 120 p.
35. **Andre Lomaka.** Biomedical applications of predictive computational chemistry. Tartu, 2003. 132 p.
36. **Kostyantyn Kirichenko.** Benzotriazole – Mediated Carbon–Carbon Bond Formation. Tartu, 2003. 132 p.
37. **Gunnar Nurk.** Adsorption kinetics of some organic compounds on bismuth single crystal electrodes. Tartu, 2003, 170 p.
38. **Mati Arulepp.** Electrochemical characteristics of porous carbon materials and electrical double layer capacitors. Tartu, 2003, 196 p.
39. **Dan Cornel Fara.** QSPR modeling of complexation and distribution of organic compounds. Tartu, 2004, 126 p.
40. **Riina Mahlapuu.** Signalling of galanin and amyloid precursor protein through adenylate cyclase. Tartu, 2004, 124 p.

41. **Mihkel Kerikmäe.** Some luminescent materials for dosimetric applications and physical research. Tartu, 2004, 143 p.
42. **Jaanus Kruusma.** Determination of some important trace metal ions in human blood. Tartu, 2004, 115 p.
43. **Urmas Johanson.** Investigations of the electrochemical properties of polypyrrole modified electrodes. Tartu, 2004, 91 p.
44. **Kaido Sillar.** Computational study of the acid sites in zeolite ZSM-5. Tartu, 2004, 80 p.
45. **Aldo Oras.** Kinetic aspects of dATPαS interaction with $P2Y_1$ receptor. Tartu, 2004, 75 p.
46. **Erik Mölder.** Measurement of the oxygen mass transfer through the air-water interface. Tartu, 2005, 73 p.
47. **Thomas Thomberg.** The kinetics of electroreduction of peroxodisulfate anion on cadmium (0001) single crystal electrode. Tartu, 2005, 95 p.
48. **Olavi Loog.** Aspects of condensations of carbonyl compounds and their imine analogues. Tartu, 2005, 83 p.
49. **Siim Salmar.** Effect of ultrasound on ester hydrolysis in aqueous ethanol. Tartu, 2006, 73 p.
50. **Ain Uustare.** Modulation of signal transduction of heptahelical receptors by other receptors and G proteins. Tartu, 2006, 121 p.
51. **Sergei Yurchenko.** Determination of some carcinogenic contaminants in food. Tartu, 2006, 143 p.
52. **Kaido Tämm.** QSPR modeling of some properties of organic compounds. Tartu, 2006, 67 p.
53. **Olga Tšubrik.** New methods in the synthesis of multisubstituted hydrazines. Tartu. 2006, 183 p.
54. **Lilli Sooväli.** Spectrophotometric measurements and their uncertainty in chemical analysis and dissociation constant measurements. Tartu, 2006, 125 p.
55. **Eve Koort.** Uncertainty estimation of potentiometrically measured ph and pK_a values. Tartu, 2006, 139 p.
56. **Sergei Kopanchuk.** Regulation of ligand binding to melanocortin receptor subtypes. Tartu, 2006, 119 p.
57. **Silvar Kallip.** Surface structure of some bismuth and antimony single crystal electrodes. Tartu, 2006, 107 p.
58. **Kristjan Saal.** Surface silanization and its application in biomolecule coupling. Tartu, 2006, 77 p.
59. **Tanel Tätte.** High viscosity $Sn(OBu)_4$ oligomeric concentrates and their applications in technology. Tartu, 2006, 91 p.
60. **Dimitar Atanasov Dobchev**. Robust QSAR methods for the prediction of properties from molecular structure. Tartu, 2006, 118 p.
61. **Hannes Hagu**. Impact of ultrasound on hydrophobic interactions in solutions. Tartu, 2007, 81 p.
62. **Rutha Jäger.** Electroreduction of peroxodisulfate anion on bismuth electrodes. Tartu, 2007, 142 p.

63. **Kaido Viht.** Immobilizable bisubstrate-analogue inhibitors of basophilic protein kinases: development and application in biosensors. Tartu, 2007, 88 p.
64. **Eva-Ingrid Rõõm.** Acid-base equilibria in nonpolar media. Tartu, 2007, 156 p.
65. **Sven Tamp.** DFT study of the cesium cation containing complexes relevant to the cesium cation binding by the humic acids. Tartu, 2007, 102 p.
66. **Jaak Nerut.** Electroreduction of hexacyanoferrate(III) anion on Cadmium (0001) single crystal electrode. Tartu, 2007, 180 p.
67. **Lauri Jalukse.** Measurement uncertainty estimation in amperometric dissolved oxygen concentration measurement. Tartu, 2007, 112 p.
68. **Aime Lust.** Charge state of dopants and ordered clusters formation in CaF_2:Mn and CaF_2:Eu luminophors. Tartu, 2007, 100 p.
69. **Iiris Kahn**. Quantitative Structure-Activity Relationships of environmentally relevant properties. Tartu, 2007, 98 p.
70. **Mari Reinik.** Nitrates, nitrites, N-nitrosamines and polycyclic aromatic hydrocarbons in food: analytical methods, occurrence and dietary intake. Tartu, 2007, 172 p.
71. **Heili Kasuk.** Thermodynamic parameters and adsorption kinetics of organic compounds forming the compact adsorption layer at Bi single crystal electrodes. Tartu, 2007, 212 p.
72. **Erki Enkvist.** Synthesis of adenosine-peptide conjugates for biological applications. Tartu, 2007, 114 p.
73. **Svetoslav Hristov Slavov**. Biomedical applications of the QSAR approach. Tartu, 2007, 146 p.
74. **Eneli Härk.** Electroreduction of complex cations on electrochemically polished Bi(*hkl*) single crystal electrodes. Tartu, 2008, 158 p.
75. **Priit Möller.** Electrochemical characteristics of some cathodes for medium temperature solid oxide fuel cells, synthesized by solid state reaction technique. Tartu, 2008, 90 p.
76. **Signe Viggor.** Impact of biochemical parameters of genetically different pseudomonads at the degradation of phenolic compounds. Tartu, 2008, 122 p.
77. **Ave Sarapuu.** Electrochemical reduction of oxygen on quinone-modified carbon electrodes and on thin films of platinum and gold. Tartu, 2008, 134 p.
78. **Agnes Kütt.** Studies of acid-base equilibria in non-aqueous media. Tartu, 2008, 198 p.
79. **Rouvim Kadis.** Evaluation of measurement uncertainty in analytical chemistry: related concepts and some points of misinterpretation. Tartu, 2008, 118 p.
80. **Valter Reedo.** Elaboration of IVB group metal oxide structures and their possible applications. Tartu, 2008, 98 p.
81. **Aleksei Kuznetsov.** Allosteric effects in reactions catalyzed by the cAMP-dependent protein kinase catalytic subunit. Tartu, 2009, 133 p.

82. **Aleksei Bredihhin.** Use of mono- and polyanions in the synthesis of multisubstituted hydrazine derivatives. Tartu, 2009, 105 p.
83. **Anu Ploom.** Quantitative structure-reactivity analysis in organosilicon chemistry. Tartu, 2009, 99 p.
84. **Argo Vonk.** Determination of adenosine A_{2A}- and dopamine D_1 receptor-specific modulation of adenylate cyclase activity in rat striatum. Tartu, 2009, 129 p.
85. **Indrek Kivi.** Synthesis and electrochemical characterization of porous cathode materials for intermediate temperature solid oxide fuel cells. Tartu, 2009, 177 p.
86. **Jaanus Eskusson.** Synthesis and characterisation of diamond-like carbon thin films prepared by pulsed laser deposition method. Tartu, 2009, 117 p.
87. **Marko Lätt.** Carbide derived microporous carbon and electrical double layer capacitors. Tartu, 2009, 107 p.
88. **Vladimir Stepanov.** Slow conformational changes in dopamine transporter interaction with its ligands. Tartu, 2009, 103 p.
89. **Aleksander Trummal.** Computational Study of Structural and Solvent Effects on Acidities of Some Brønsted Acids. Tartu, 2009, 103 p.
90. **Eerold Vellemäe.** Applications of mischmetal in organic synthesis. Tartu, 2009, 93 p.
91. **Sven Parkel.** Ligand binding to 5-HT_{1A} receptors and its regulation by Mg^{2+} and Mn^{2+}. Tartu, 2010, 99 p.
92. **Signe Vahur.** Expanding the possibilities of ATR-FT-IR spectroscopy in determination of inorganic pigments. Tartu, 2010, 184 p.
93. **Tavo Romann**. Preparation and surface modification of bismuth thin film, porous, and microelectrodes. Tartu, 2010, 155 p.
94. **Nadežda Aleksejeva.** Electrocatalytic reduction of oxygen on carbon nanotube-based nanocomposite materials. Tartu, 2010, 147 p.
95. **Marko Kullapere.** Electrochemical properties of glassy carbon, nickel and gold electrodes modified with aryl groups. Tartu, 2010, 233 p.
96. **Liis Siinor.** Adsorption kinetics of ions at Bi single crystal planes from aqueous electrolyte solutions and room-temperature ionic liquids. Tartu, 2010, 101 p.
97. **Angela Vaasa.** Development of fluorescence-based kinetic and binding assays for characterization of protein kinases and their inhibitors. Tartu 2010, 101 p.
98. **Indrek Tulp.** Multivariate analysis of chemical and biological properties. Tartu 2010, 105 p.
99. **Aare Selberg.** Evaluation of environmental quality in Northern Estonia by the analysis of leachate. Tartu 2010, 117 p.
100. **Darja Lavõgina.** Development of protein kinase inhibitors based on adenosine analogue-oligoarginine conjugates. Tartu 2010, 248 p.
101. **Laura Herm.** Biochemistry of dopamine D_2 receptors and its association with motivated behaviour. Tartu 2010, 156 p.

102. **Terje Raudsepp.** Influence of dopant anions on the electrochemical properties of polypyrrole films. Tartu 2010, 112 p.
103. **Margus Marandi.** Electroformation of Polypyrrole Films: *In-situ* AFM and STM Study. Tartu 2011, 116 p.
104. **Kairi Kivirand.** Diamine oxidase-based biosensors: construction and working principles. Tartu, 2011, 140 p.
105. **Anneli Kruve.** Matrix effects in liquid-chromatography electrospray mass-spectrometry. Tartu, 2011, 156 p.
106. **Gary Urb.** Assessment of environmental impact of oil shale fly ash from PF and CFB combustion. Tartu, 2011, 108 p.
107. **Nikita Oskolkov.** A novel strategy for peptide-mediated cellular delivery and induction of endosomal escape. Tartu, 2011, 106 p.
108. **Dana Martin.** The QSPR/QSAR approach for the prediction of properties of fullerene derivatives. Tartu, 2011, 98 p.
109. **Säde Viirlaid.** Novel glutathione analogues and their antioxidant activity. Tartu, 2011, 106 p.
110. **Ülis Sõukand.** Simultaneous adsorption of Cd^{2+}, Ni^{2+}, and Pb^{2+} on peat. Tartu, 2011, 124 p.
111. **Lauri Lipping.** The acidity of strong and superstrong Brønsted acids, an outreach for the "limits of growth": a quantum chemical study. Tartu, 2011, 124 p.
112. **Heisi Kurig.** Electrical double-layer capacitors based on ionic liquids as electrolytes. Tartu, 2011, 146 p.
113. **Marje Kasari.** Bisubstrate luminescent probes, optical sensors and affinity adsorbents for measurement of active protein kinases in biological samples. Tartu, 2012, 126 p.
114. **Kalev Takkis.** Virtual screening of chemical databases for bioactive molecules. Tartu, 2012, 122 p.
115. **Ksenija Kisseljova**. Synthesis of aza-β^3-amino acid containing peptides and kinetic study of their phosphorylation by protein kinase A. Tartu, 2012, 104 p.
116. **Riin Rebane.** Advanced method development strategy for derivatization LC/ESI/MS. Tartu, 2012, 184 p.
117. **Vladislav Ivaništšev.** Double layer structure and adsorption kinetics of ions at metal electrodes in room temperature ionic liquids. Tartu, 2012, 128 p.
118. **Irja Helm.** High accuracy gravimetric Winkler method for determination of dissolved oxygen. Tartu, 2012, 139 p.
119. **Karin Kipper.** Fluoroalcohols as Components of LC-ESI-MS Eluents: Usage and Applications. Tartu, 2012, 164 p.
120. **Arno Ratas.** Energy storage and transfer in dosimetric luminescent materials. Tartu, 2012, 163 p.
121. **Reet Reinart-Okugbeni**. Assay systems for characterisation of subtype-selective binding and functional activity of ligands on dopamine receptors. Tartu, 2012, 159 p.

122. **Lauri Sikk.** Computational study of the Sonogashira cross-coupling reaction. Tartu, 2012, 81 p.
123. **Karita Raudkivi.** Neurochemical studies on inter-individual differences in affect-related behaviour of the laboratory rat. Tartu, 2012, 161 p.
124. **Indrek Saar.** Design of GalR2 subtype specific ligands: their role in depression-like behavior and feeding regulation. Tartu, 2013, 126 p.
125. **Ann Laheäär.** Electrochemical characterization of alkali metal salt based non-aqueous electrolytes for supercapacitors. Tartu, 2013, 127 p.
126. **Kerli Tõnurist.** Influence of electrospun separator materials properties on electrochemical performance of electrical double-layer capacitors. Tartu, 2013, 147 p.
127. **Kaija Põhako-Esko.** Novel organic and inorganic ionogels: preparation and characterization. Tartu, 2013, 124 p.
128. **Ivar Kruusenberg.** Electroreduction of oxygen on carbon nanomaterial-based catalysts. Tartu, 2013, 191 p.
129. **Sander Piiskop.** Kinetic effects of ultrasound in aqueous acetonitrile solutions. Tartu, 2013, 95 p.
130. **Ilona Faustova**. Regulatory role of L-type pyruvate kinase N-terminal domain. Tartu, 2013, 109 p.
131. **Kadi Tamm.** Synthesis and characterization of the micro-mesoporous anode materials and testing of the medium temperature solid oxide fuel cell single cells. Tartu, 2013, 138 p.
132. **Iva Bozhidarova Stoyanova-Slavova.** Validation of QSAR/QSPR for regulatory purposes. Tartu, 2013, 109 p.
133. **Vitali Grozovski**. Adsorption of organic molecules at single crystal electrodes studied by *in situ* STM method. Tartu, 2014, 146 p.
134. **Santa Veikšina**. Development of assay systems for characterisation of ligand binding properties to melanocortin 4 receptors. Tartu, 2014, 151 p.
135. **Jüri Liiv.** PVDF (polyvinylidene difluoride) as material for active element of twisting-ball displays. Tartu, 2014, 111 p.
136. **Kersti Vaarmets.** Electrochemical and physical characterization of pristine and activated molybdenum carbide-derived carbon electrodes for the oxygen electroreduction reaction. Tartu, 2014, 131 p.
137. **Lauri Tõntson**. Regulation of G-protein subtypes by receptors, guanine nucleotides and Mn^{2+}. Tartu, 2014, 105 p.
138. **Aiko Adamson.** Properties of amine-boranes and phosphorus analogues in the gas phase. Tartu, 2014, 78 p.
139. **Elo Kibena**. Electrochemical grafting of glassy carbon, gold, highly oriented pyrolytic graphite and chemical vapour deposition-grown graphene electrodes by diazonium reduction method. Tartu, 2014, 184 p.
140. **Teemu Näykki.** Novel Tools for Water Quality Monitoring – From Field to Laboratory. Tartu, 2014, 202 p.
141. **Karl Kaupmees.** Acidity and basicity in non-aqueous media: importance of solvent properties and purity. Tartu, 2014, 128 p.

142. **Oleg Lebedev**. Hydrazine polyanions: different strategies in the synthesis of heterocycles. Tartu, 2015, 118 p.
143. **Geven Piir.** Environmental risk assessment of chemicals using QSAR methods. Tartu, 2015, 123 p.
144. **Olga Mazina.** Development and application of the biosensor assay for measurements of cyclic adenosine monophosphate in studies of G protein-coupled receptor signalinga. Tartu, 2015, 116 p.
145. **Sandip Ashokrao Kadam.** Anion receptors: synthesis and accurate binding measurements. Tartu, 2015, 116 p.
146. **Indrek Tallo.** Synthesis and characterization of new micro-mesoporous carbide derived carbon materials for high energy and power density electrical double layer capacitors. Tartu, 2015, 148 p.
147. **Heiki Erikson.** Electrochemical reduction of oxygen on nanostructured palladium and gold catalysts. Tartu, 2015, 204 p.
148. **Erik Anderson.** *In situ* Scanning Tunnelling Microscopy studies of the interfacial structure between Bi(111) electrode and a room temperature ionic liquid. Tartu, 2015, 118 p.
149. **Girinath G. Pillai.** Computational Modelling of Diverse Chemical, Biochemical and Biomedical Properties. Tartu, 2015, 140 p.
150. **Piret Pikma.** Interfacial structure and adsorption of organic compounds at Cd(0001) and Sb(111) electrodes from ionic liquid and aqueous electrolytes: an *in situ* STM study. Tartu, 2015, 126 p.
151. **Ganesh babu Manoharan.** Combining chemical and genetic approaches for photoluminescence assays of protein kinases. Tartu, 2016, 126 p.
152. **Carolin Siimenson**. Electrochemical characterization of halide ion adsorption from liquid mixtures at Bi(111) and pyrolytic graphite electrode surface. Tartu, 2016, 110 p.
153. **Asko Laaniste.** Comparison and optimisation of novel mass spectrometry ionisation sources. Tartu, 2016, 156 p.
154. **Hanno Evard.** Estimating limit of detection for mass spectrometric analysis methods. Tartu, 2016, 224 p.
155. **Kadri Ligi.** Characterization and application of protein kinase-responsive organic probes with triplet-singlet energy transfer. Tartu, 2016, 122 p.
156. **Margarita Kagan.** Biosensing penicillins' residues in milk flows. Tartu, 2016, 130 p.
157. **Marie Kriisa.** Development of protein kinase-responsive photoluminescent probes and cellular regulators of protein phosphorylation. Tartu, 2016, 106 p.
158. **Mihkel Vestli.** Ultrasonic spray pyrolysis deposited electrolyte layers for intermediate temperature solid oxide fuel cells. Tartu, 2016, 156 p.
159. **Silver Sepp**. Influence of porosity of the carbide-derived carbon on the properties of the composite electrocatalysts and characteristics of polymer electrolyte fuel cells. Tartu, 2016, 137 p.
160. **Kristjan Haav**. Quantitative relative equilibrium constant measurements in supramolecular chemistry. Tartu, 2017, 158 p.

161. **Anu Teearu**. Development of MALDI-FT-ICR-MS methodology for the analysis of resinous materials. Tartu, 2017, 205 p.
162. **Taavi Ivan**. Bifunctional inhibitors and photoluminescent probes for studies on protein complexes. Tartu, 2017, 140 p.
163. **Maarja-Liisa Oldekop**. Characterization of amino acid derivatization reagents for LC-MS analysis. Tartu, 2017, 147 p.
164. **Kristel Jukk**. Electrochemical reduction of oxygen on platinum- and palladium-based nanocatalysts. Tartu, 2017, 250 p.
165. **Siim Kukk**. Kinetic aspects of interaction between dopamine transporter and *N*-substituted nortropane derivatives. Tartu, 2017, 107 p.
166. **Birgit Viira**. Design and modelling in early drug development in targeting HIV-1 reverse transcriptase and Malaria. Tartu, 2017, 172 p.
167. **Rait Kivi**. Allostery in cAMP dependent protein kinase catalytic subunit. Tartu, 2017, 115 p.
168. **Agnes Heering**. Experimental realization and applications of the unified acidity scale. Tartu, 2017, 123 p.
169. **Delia Juronen**. Biosensing system for the rapid multiplex detection of mastitis-causing pathogens in milk. Tartu, 2018, 85 p.
170. **Hedi Rahnel.** ARC-inhibitors: from reliable biochemical assays to regulators of physiology of cells. Tartu, 2018, 176 p.
171. **Anton Ruzanov.** Computational investigation of the electrical double layer at metal–aqueous solution and metal–ionic liquid interfaces. Tartu, 2018, 129 p.
172. **Katrin Kestav.** Crystal Structure-Guided Development of Bisubstrate-Analogue Inhibitors of Mitotic Protein Kinase Haspin. Tartu, 2018, 166 p.
173. **Mihkel Ilisson.** Synthesis of novel heterocyclic hydrazine derivatives and their conjugates. Tartu, 2018, 101 p.
174. **Anni Allikalt.** Development of assay systems for studying ligand binding to dopamine receptors. Tartu, 2018, 160 p.
175. **Ove Oll.** Electrical double layer structure and energy storage characteristics of ionic liquid based capacitors. Tartu, 2018, 187 p.
176. **Rasmus Palm.** Carbon materials for energy storage applications. Tartu, 2018, 114 p.
177. **Jörgen Metsik.** Preparation and stability of poly(3,4-ethylenedioxythiophene) thin films for transparent electrode applications. Tartu, 2018, 111 p.
178. **Sofja Tšepelevitš.** Experimental studies and modeling of solute-solvent interactions. Tartu, 2018, 109 p.
179. **Märt Lõkov.** Basicity of some nitrogen, phosphorus and carbon bases in acetonitrile. Tartu, 2018, 104 p.
180. **Anton Mastitski**. Preparation of α-aza-amino acid precursors and related compounds by novel methods of reductive one-pot alkylation and direct alkylation. Tartu, 2018, 155 p.
181. **Jürgen Vahter**. Development of bisubstrate inhibitors for protein kinase CK2. Tartu, 2019, 186 p.

182. **Piia Liigand.** Expanding and improving methodology and applications of ionization efficiency measurements. Tartu, 2019, 189 p.
183. **Sigrid Selberg.** Synthesis and properties of lipophilic phosphazene-based indicator molecules. Tartu, 2019, 74 p.
184. **Jaanus Liigand.** Standard substance free quantification for LC/ESI/MS analysis based on the predicted ionization efficiencies. Tartu, 2019, 254 p.
185. **Marek Mooste.** Surface and electrochemical characterisation of aryl film and nanocomposite material modified carbon and metal-based electrodes. Tartu, 2019, 304 p.
186. **Mare Oja.** Experimental investigation and modelling of pH profiles for effective membrane permeability of drug substances. Tartu, 2019, 306 p.
187. **Sajid Hussain.** Electrochemical reduction of oxygen on supported Pt catalysts. Tartu, 2019, 220 p.
188. **Ronald Väli.** Glucose-derived hard carbon electrode materials for sodium-ion batteries. Tartu, 2019, 180 p.
189. **Ester Tee.** Analysis and development of selective synthesis methods of hierarchical micro- and mesoporous carbons. Tartu, 2019, 210 p.
190. **Martin Maide.** Influence of the microstructure and chemical composition of the fuel electrode on the electrochemical performance of reversible solid oxide fuel cell. Tartu, 2020, 144 p.
191. **Edith Viirlaid.** Biosensing Pesticides in Water Samples. Tartu, 2020, 102 p.
192. **Maike Käärik.** Nanoporous carbon: the controlled nanostructure, and structure-property relationships. Tartu, 2020, 162 p.
193. **Artur Gornischeff.** Study of ionization efficiencies for derivatized compounds in LC/ESI/MS and their application for targeted analysis. Tartu, 2020, 124 p.
194. **Reet Link.** Ligand binding, allosteric modulation and constitutive activity of melanocortin-4 receptors. Tartu, 2020, 108 p.
195. **Pilleriin Peets.** Development of instrumental methods for the analysis of textile fibres and dyes. Tartu, 2020, 150 p.
196. **Larisa Ivanova.** Design of active compounds against neurodegenerative diseases. Tartu, 2020, 152 p.
197. **Meelis Härmas.** Impact of activated carbon microstructure and porosity on electrochemical performance of electrical double-layer capacitors. Tartu, 2020, 122 p.
198. **Ruta Hecht.** Novel Eluent Additives for LC-MS Based Bioanalytical Methods. Tartu, 2020, 202 p.
199. **Max Hecht.** Advances in the Development of a Point-of-Care Mass Spectrometer Test. Tartu, 2020, 168 p.
200. **Ida Rahu.** Bromine formation in inorganic bromide/nitrate mixtures and its application for oxidative aromatic bromination. Tartu, 2020, 116 p.
201. **Sander Ratso**. Electrocatalysis of oxygen reduction on non-precious metal catalysts. Tartu, 2020, 371 p.
202. **Astrid Darnell.** Computational design of anion receptors and evaluation of host-guest binding. Tartu, 2021, 150 p.

203. **Ove Korjus.** The development of ceramic fuel electrode for solid oxide cells. Tartu, 2021, 150 p.
204. **Merit Oss.** Ionization efficiency in electrospray ionization source and its relations to compounds' physico-chemical properties. Tartu, 2021, 124 p.
205. **Madis Lüsi**. Electroreduction of oxygen on nanostructured palladium catalysts. Tartu, 2021, 180 p.
206. **Eliise Tammekivi.** Derivatization and quantitative gas-chromatographic analysis of oils. Tartu, 2021, 122 p.
207. **Simona Selberg.** Development of Small-Molecule Regulators of Epitranscriptomic Processes. Tartu, 2021, 122 p.
208. **Olivier Etebe Nonga.** Inhibitors and photoluminescent probes for in vitro studies on protein kinases PKA and PIM. Tartu, 2021, 189 p.
209. **Riinu Härmas.** The structure and H2 diffusion in porous carbide-derived carbon particles. Tartu, 2022, 123 p.
210. **Maarja Paalo.** Synthesis and characterization of novel carbon electrodes for high power density electrochemical capacitors. Tartu, 2022, 144 p.
211. **Jinfeng Zhao.** Electrochemical characteristics of Bi(hkl) and micro-mesoporous carbon electrodes in ionic liquid based electrolytes. Tartu, 2022, 134 p.
212. **Alar Heinsaar.** Investigation of oxygen electrode materials for high-temperature solid oxide cells in natural conditions. Tartu, 2022, 120 p.
213. **Jaana Lilloja.** Transition metal and nitrogen doped nanocarbon cathode catalysts for anion exchange membrane fuel cells. Tartu, 2022, 202 p.
214. **Maris-Johanna Tahk.** Novel fluorescence-based methods for illuminating transmembrane signal transduction by G-protein coupled receptors. Tartu, 2022, 200 p.
215. **Eerik Jõgi.** Development and Applications of E. coli Immunosensor. Tartu, 2022, 103 p.
216. **Alo Rüütel.** Design principles of synthetic molecular receptors for anion-selective electrodes. Tartu, 2022, 109 p.
217. **Tanel Sõrmus.** Development of stimuli-responsive and covalent bisubstrate inhibitors of protein kinases. Tartu, 2022, 148 p.
218. **Oleg Artemchuk.** Autotrophic nitrogen removal processes for nutrient removal from sidestream and mainstream wastewater. Tartu, 2022, 115 p.